DANMARKS OG GRØNLANDS GEOLOGISKE UNDERSØGELSE RAPPORT 2001/35

Geological Settings and Fracture Distribution on a Granite site in Nothern Spain

TRACe-Fracture
Toward an Improved Risk Assessment of the Contaminant Spreading in Fractured Underground Reservoirs
Progress report

K.E.S. Klint, F. Sanchez, P. Gravesen & L. Molinelli

GEOLOGICAL SURVEY OF DENMARK AND GREENLAND
MINISTRY OF ENVIRONMENT AND ENERGY

G E U S

DANMARKS OG GRØNLANDS GEOLOGISKE UNDERSØGELSE RAPPORT 2001/35

Geological Settings and Fracture Distribution on a Granite site in Nothern Spain

TRACe-Fracture
Toward an Improved Risk Assessment of the Contaminant Spreading in Fractured Underground Reservoirs
Progress report

K.E.S. Klint, F. Sanchez, P. Gravesen and L. Molinelli

GEOLOGICAL SURVEY OF DENMARK AND GREENLAND
MINISTRY OF ENVIRONMENT AND ENERGY

GEUS

Content

1. Introduction

This report was written as part of the GEUS deliveries for in the EU-project EVK1-CT1999-00013: TRACE-FRACTURE (Toward an Improved Risk Assessment of the Contaminant Spreading in Fractured Underground Reservoirs). A detailed geological investigation has been carried out on a location in Northern Spain characterised by fractured granitic rocks.
The primary purpose of this report is to analyse the distribution of fractures in the area and construct a conceptual fracture model for the area. Based on the fracture model samples of representative fractures has been collected for detailed analysis of their topological and hydraulic properties.

This report is no. 1 of 4 annual progress reports containing the deliveries from GEUS in task 1-1, 1-2 and 1-3. The reports are:

1. Klint K.E.S., Francisco S., Gravesen P. and Molinelli L., 2001: Geological Settings and Fracture Distribution on a Granite site in Northern Spain. In: TRACe-Fracture. Toward an Improved Risk Assessment of the Contaminant Spreading in Fractured Underground Reservoirs. GEUS Progress report no 35.

2. Klint K.E.S., Rosenbom A. and Gravesen P. 2001: Geological Setting and Fracture Distribution on a Clay Till site in Ringe, Denmark. In: TRACe-Fracture. Toward an Improved Risk Assessment of the Contaminant Spreading in Fractured Underground Reservoirs. GEUS Progress report no 36.

3. Rosenbom A. Hansen M., and Klint K.E.S., 2001. Image and SEM-analysis of Fractures and Pore Structures in Clay Till. In: TRACe-Fracture. Toward an Improved Risk Assessment of the Contaminant Spreading in Fractured Underground Reservoirs. GEUS Progress report no 37.

4. Rosenbom A.E., Hansen M., Klint K.E.S.K., Lorentzen H.J. and Springer N. 2001: Image and SEM-analysis of Fractures in Granite. In: TRACe-Fracture. Toward an Improved Risk Assessment of the Contaminant Spreading in Fractured Underground Reservoirs. GEUS Progress report no 38.

2. Goals and Scopes

The goal of this task was to investigate a fractured granite site in Northern Spain and construct a geological model in combination with a fracture model representing an example of a fractured granite site. Combined with detailed analysis of possible contaminant transport in the fractured granite, this data should form the basis for the construction of a Risk Assessment model that can simulate transport and spreading of contaminants in fractured underground reservoirs.

A full investigation of fractures includes:

- Reconstruction of the tectonic history of the area
- Classification and characterisation of the fractures into fracture systems with characteristic properties.
- Calculation of quantitative fracture properties for each fracture system, primarily spacing of the individual fracture systems and measurement of the mechanical fracture aperture (opening diameter).
- Hydraulic tests of fractures, either from wells or in core samples.

This report focus exclusively on the description of the tectonic history of the area, analysis of the fracture distribution, classification of fractures into distinct fracture systems and finally calculation of the quantitative fracture properties. This forms the base for the construction of a conceptual fracture model, while descriptions of the hydraulic analysis and fracture flow properties are being presented in another report (Rosenbom et al 2001b).

3. Geological settings

The area is situated near the Atlantic coast in Northern Spain (Figure 1.1). The investigated area covers an area of approximately 6 km^2. A valley truncate the area from north-west towards south-east and separates to distinct hills of which the northern hill is approximately 200 m high while the southern hill raises to a maximum height of 243 m above sea level. Another valley, with a south-west north-east trend, is situated east of the southern hill, and meets the main valley in the central part of the area.

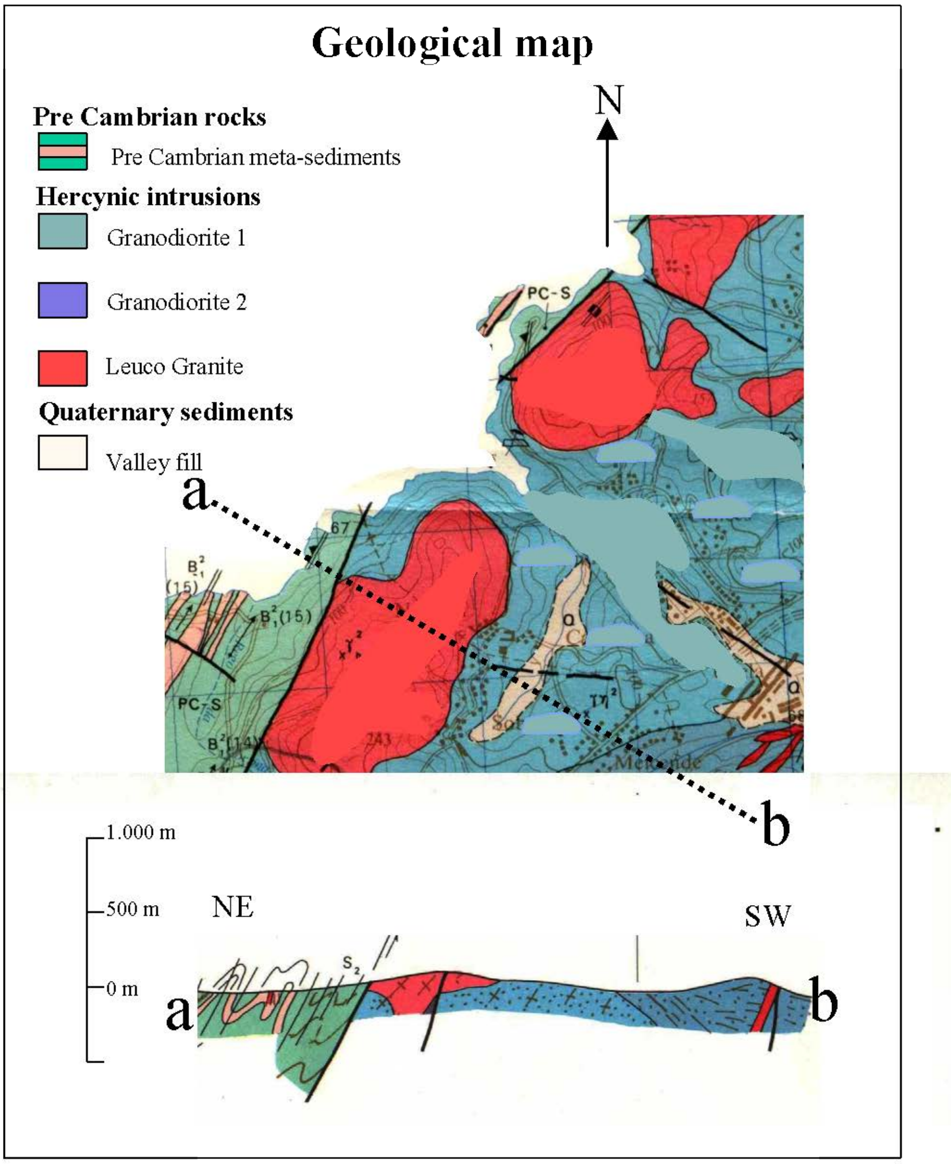

Figure 1.1.Geological map of the area with cross-section outlining the primary structures.

The Region is highly dominated by meta-sedimentary rocks of Pre-Cambrian age which have been intensively folded and intruded by rocks of primarily granitic origin during the

Hercynic fold phase from Early Devonian to Early Permian time. The Pre-Cambrian meta-sediments are dominating the western part of the area. The meta sediments consists of conglomerates and quarzites which is locally intruded by amfibolite. The rocks are separated from the Carboniferous intrusions by a large thrust-fault (figure 1.1), that truncate the area from south-west to north-east and dips towards north-west.

Two different rocks of granitic composition dominate the area east of the thrust fault, namely two different intrusions of granodiorite, and a fine-grained leucogranite (figure 1.1).

The leucogranite is a light brown crystalline rock with a large content of mica (muscovite), quartz and feldspar. Some dark minerals gives the leucogranite a foliated appearance on some sites, while it is rather massive on other sites. It occurs in dikes truncating the granodiorite and in a large body (a lacolith) covering the granodiorite intrusion.

The granodiorite 1 is a coarse-grained crystalline rock with quartz crystals and characteristic large feldspar crystals up to 2-3 cm long. The rock appears massive, but are locally sheared along major faults. This rock also appears heavily weathered in some regions. In this case it easily falls apart, and can be excavated and are used as roadfill.

The valley floors are covered by different types of sediments primarily sandy deposits of Quaternary age, but clayey and silty sediments appears as well.

Regional Geological history.

The geological history of northern Spain is highly affected by the formation of the Super continent Pangea in the socalled Hercynic orogenic phse that took place 400-250 MA. Spain was situated between the two continents Laurussia and Gondwanaland in Silurian. In late Silurian (~410-390 MA.) the Iberian Peninsula drifted towards Laurussia closing the Merrimack Ocean. In Middle Devonian the Ocean had closed and Iberia had merged with Laurussia. At the same time Gondwanaland to the south was drifting north slowly closing the Proto-Atlantic and Thethys Ocean. The Iberian Peninsula was deformed and the central Iberian Foldbelt was formed in a zone of dominating dextral transform shear (Ziegler 1989). During Carboniferous (335-310 MA.) the Variscian Orogeny culminated and especially dextral transform shear deformation prevailed in the Iberian area as Gondwanaland rotated in a dextral clockwise manner. During this period large granite bodies intruded the Pre-Cambrian folded meta sediments. After the Carboniferous locking of the Hercynian subduction system, the contact-zone or mega-suture between Laurussia and Gondwanaland consolidated in the Early Permian period, and the Super-continent Pangea was formed. The region was in general uplifted during the Permian and around the Late Permian-Early Triassian period (250 MA.) a gradual development of a regional tensional regime was reflected by development of new rift-zones and reactivation of older Permo-Carboniferous fault systems. Later these rift-zones joined into the Mid-Atlantic rift zone, splitting of the Super continent and forming the Atlantic Ocean. The geological map (figure 1.2) shows the distribution of rocks in north western Spain and the following text are relating to some of these rocks especially the granodirite 2 (figure 1.2).

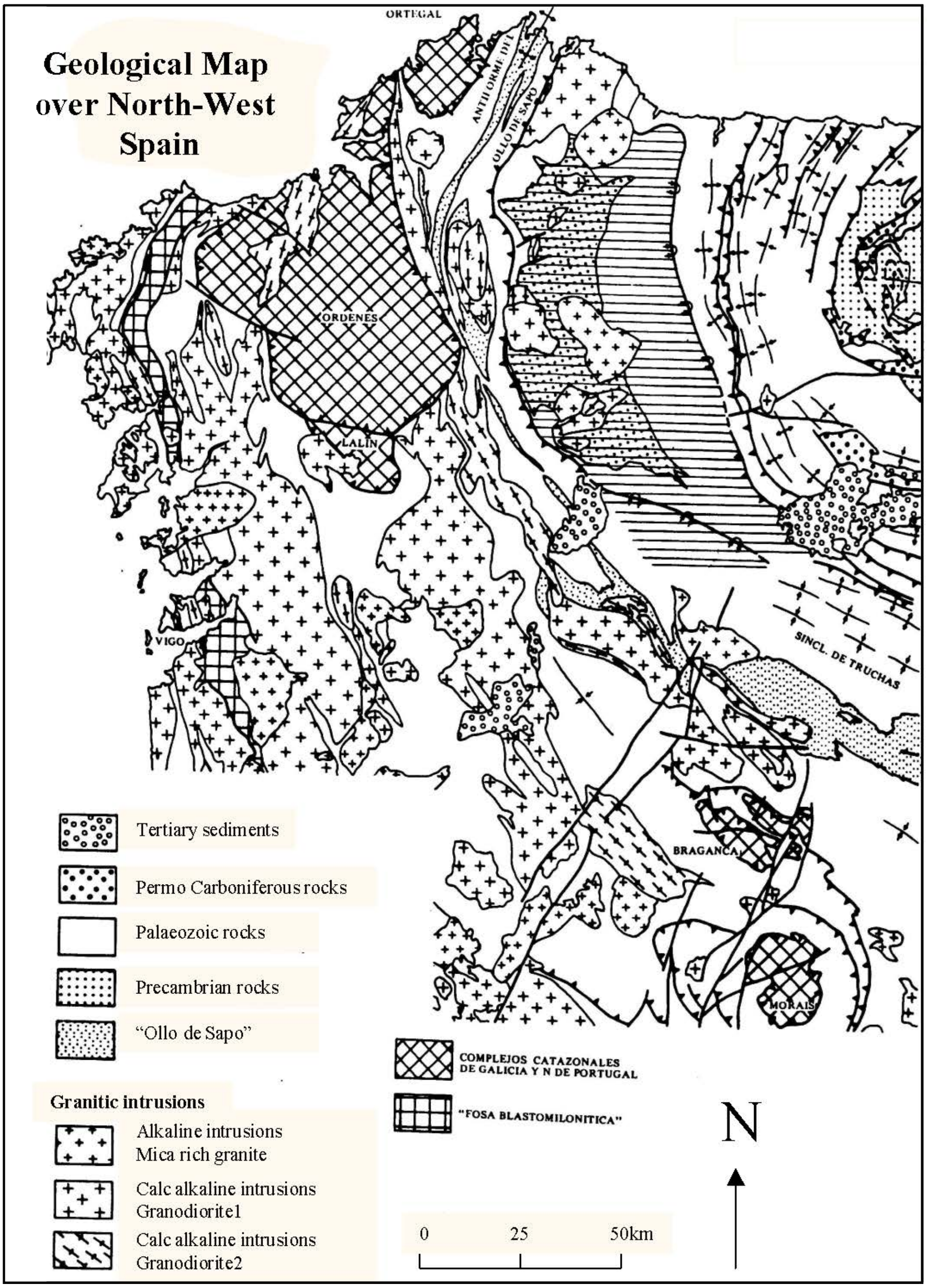

Figure 1.2. Regional geological map of north western Spain.

4. Methods

Characterisation of fractures includes a full scale geological investigation, as the distributions of the fractures are closely related to the rock-mechanics and the tectonic history of the area. Fractures in non-stratabound rocks such as intrusive rocks are in general very different from fractures in stratabound rocks such as sandstone or limestone. Attempts to construct a regional conceptual fracture model depends thus on the number and quality of the field data.

A number of selected outcrops with large and well exposed fractures were selected for detailed fracture analysis. Large scale analysis of fracture distributions were carried out using image analysis of Arial photos with visible fracture traces on exposed outcrops. The observations were later verified on the ground.

4.1 Fracture classification

Fractures include all brittle failures such as joints, fissures, cracks, veins, etc. which are not faults, beddings or cleavages, and which are larger than the grain size of the rock. In general fractures are defined as dominantly opening mode fractures, and as such, they are associated with characteristic stress, strain and displacement fields. They are distinguished from small faults by distinctive surface textures and lack of shear displacements. Some fractures may however show a small displacement between the two fracture surfaces, with additional development of stria or "slickensides" on the surface, and are thus referred to as shear fractures or micro-faults.

Fractures form in relation to a certain stress field, either as systematic sets of parallel fractures with a distinct orientation, or in some cases as more irregular non systematic fractures with an overall random orientation. Systematic fractures form thus “families” of fractures with special characteristics, that may be related to distinct tectonic processes. The classification of fractures is primarily based on the orientation of the fractures. Once classified as systematic or non-systematic the fracture properties may be calculated, and a more detailed classification related to other characteristics such as fracture shape and size may be included in the classification, by comparition with the characteristics of the different fracture types.

Fracture parameters.

Fracture models need generally input of fracture *position*, *orientation, size*, *density (connectivity)* and *aperture* of single fractures. The *density* or number of fractures pr volume unit, may be measured as fracture area pr volume unit, (which is very difficult to measure) or as fracture trace-length pr area unit, which can be measured, but which is generally biased. Another way is to measure or calculate the average distance between fractures in each fracture system (fracture spacing), or the number of fractures pr volume unit (fracture intensity, figure 4.1). Finally the *connectivity* of the fractures are extremely important for the bulk hydraulic properties of the area, and good outcrop maps are therefore important in order to evaluate the spatial distribution of the fractures.

A detailed description of the fracture parameters are given in the following section and an example of the calculation of the values and relation between the parameters are demonstrated in figure 4.1. Aperture data can not be measured in the field but, samples were collected for detailed measurement of the mechanical aperture in the laboratory (Klint and Tsakiroglou 2000, Rosenbom et al 2001)

Fracture Orientation is important for preferred flow-directions and for classifying the fractures into distinct fracture sets or systems. The orientation data may be illustrated in pole diagrams or pole density diagrams on a *Stereographic Projection,* (Kazi & Knill 1973) where all fractures are plotted as the pole to the fracture plane. Systematic fractures will plot in characteristic clusters and non-systematic fractures will be randomly distributed on the stereographic plot. The fracture data are normally contoured in order to visualise the fracture distribution and identify fracture systems. A Gaussian counting method (K=100) was used (Robin and Jowett 1986). This method is also useful for analysing distribution of fractures with special characteristics such as characteristic surface precipitation or slicken-sides at the fracture surfaces etc. The fracture strike may also be illustrated in a *Rose Diagram* (Nemec 1988; Davis 1984) showing the strike variation of the fractures. The latter method gives an excellent visual presentation of the fracture orientation, but it does not account for the dip and is only used on vertical/sub-vertical fractures.

Fracture Spacing (S) is the mean perpendicular distance between adjacent fractures in an almost parallel fracture set.
The best way to calculate the spacing is to measure all spacing between fractures in the same fracture-system directly in the field and calculate the mean spacing as the average distance of all the spacings as described by Bosscher & Connel (1988). This is however quite difficult to do if several different fracture systems coexists in the same place, and near wall-parallel fractures is normally biased.

Fracture Intensity (I): 1/S is the number of fractures per meter for a single set of parallel fractures.
The spacing may be illustrated as the Fracture Intensity (1/S), which is the inverse of the fracture spacing. The Fracture Intensity allows the spacing to be illustrated on a “Rose diagram” or a graph. The sum of all fractures intensities are then showing the total number of fractures in an average cubic-meter of clay termed the *Fracture Bulk Intensity* (T_{otal}).

Fracture Trace Frequency (F_t): n/Lw is the number of fracture traces per meter counted along a scan-line. This is another way to illustrate the fracture distribution both lateral and vertical. The number of fracture traces is counted along a vertical and a horizontal scan-line, attached to the face of the exposure. The method is very fast, and large amount of data may be collected thus illustrating the spatial distribution of fractures in a large volume of sediment. The method makes it furthermore possible to register the number of fractures that are too small or irregular to be measured with a compass. It must be noted that near wall parallel fractures are biased and the average numbers are typical 1,3-2 times smaller than the true Fracture Intensity.

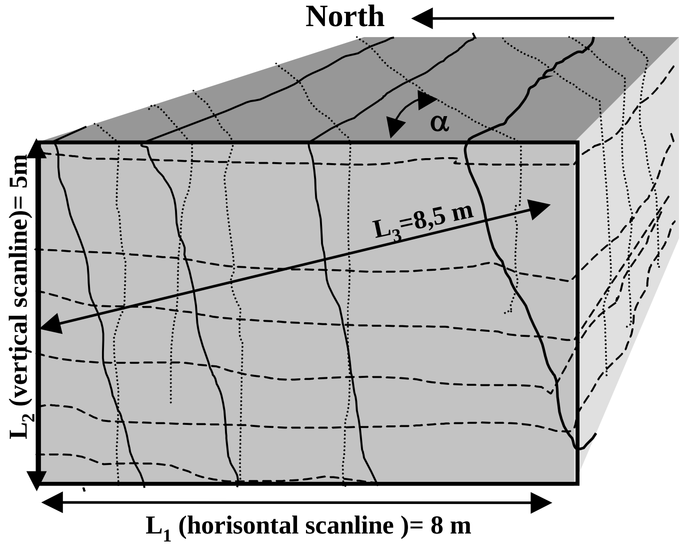

FRACTURE ORIENTATION

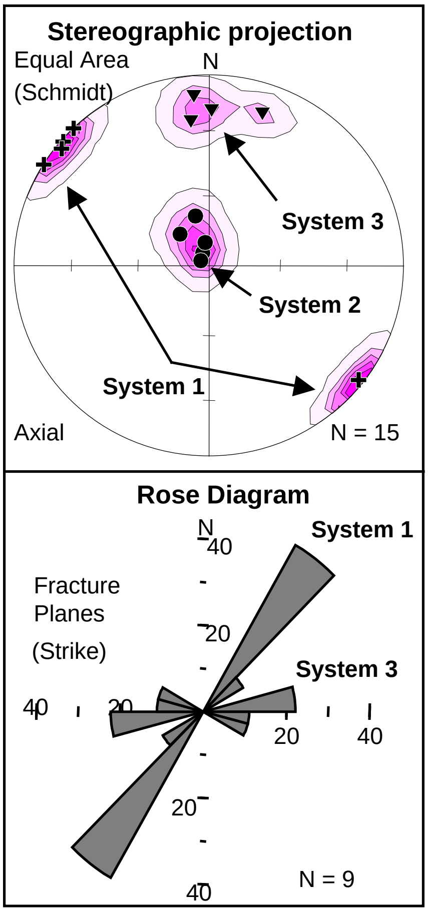

Data necessary for calculating fracture parameters
Strike of wall: 5^0
L_1 Length of horizontal scanline = 8 m
L_2 Length of vertical scanline = 5 m
L_3 Length of scanline normal to system 3 = 8,5 m
$\alpha = 35^0$ Angle between mean fracture strike for system 1 and strike of wall (Always the angle < 90^0)
Total number of fractures N = 15
System 1: Vertical fractures ✚ ············ $N_1 = 5$
System 2: Horizontal fractures ● - - - - - - - $N_2 = 6$
System 3: Oblique Fractures ▼ ———— $N_3 = 4$

Fracture Spacing (S)	**Mean distance between fractures in one set of parallel fractures**	
Spacing System 1(S_1):	Sin α x $((L_1/(N_1+1)+(L_1/(N_1-1))/2=$	
	S = Sin (35) x ((8/(5+1)+(8/(5-1))/2 = 0.96 m	
Spacing System 2(S_2):	$((L_2/(N_2+1)+(L_2/(N_2-1))/2 =$	
(Frac. perpendicular to scanline)	S = ((6/(5+1)+6/(5-1))/2 =	= 0,86 m
Spacing System 3(S_3):	$(L_3(/(N_3+1) + L_3/(N_3-1))/2=$	
(Frac. perpendicular to scanline)	S = ((8,5/(4+1) + 8,5/(4-1))/2	= 2.27 m
Cumulative Spacing (S_{total})	$S_{total} = 1/ I_{total}$	**= 0.38 m**
Fracture Intensity (I)	**Number of fractures/ m (1/S)**	
Intensity System 1	$I_1 = 1/S_1$: 1/0.96	= 1,05 fracture/m
Intensity System 2	$I_2 = 1/S_2$: 1/0.86	= 1.16 fracture/m
Intensity System 3	$I_3 = 1/S_3$: 1/2,27	= 0,44 fracture/m
Fracture Bulk Intensity (I_{total})	$I_{total} = I_1 + I_2 + I_3$	**= 2,65 fractures/m^3**

Fracture Trace Frequency (F_t): N vertical/ L_1 + N horisontal/L_2 F_t =
(9/8)+(6/5) = 1,1 frac. traces +1.2 frac. traces /m **= 2,3 frac. traces/m**
Fracture Trace Density (D_t)
Total tracelength/area: $93m/40m^2$ (vertical plane facing west) **= 2,32 m frac. trace/m^2**

Figure 4.1 Calculation of fracture parameters on an imaginary outcrop. The figure defines some fracture parameters and illustrates how some data may be biased, if the fractures are not measured in 3 dimensions. The quality of the data are furthermore demonstrated as the spacing and Intensity values are more accurate than the trace/frequency or trace density values (modified from Klint and Fredericia 1998).

4.2 Fieldwork

The fieldwork was carried out by Knud Erik Klint (GEUS) and Francisco Sanchez (CHM2-Hill), during two weeks in June 2000. The coastal cliffs and the numerous outcrops along roads and in old quarries offered excellent possibilities for detailed investigations. A total of 9 locations were thus selected for detailed investigations of fracture distributions and a general geological mapping of the distribution of different rocks and structures were carried out. Geological informations from wells in the area were collected and these data were all included in the geological model. Dikes and faults were paid special attention since the they truncated or were truncated by different fracture systems, thus facilitating the construction of an event stratigraphical model for the area.

Fracture measurement technique

A reference line were attached to the outcrop wall. In some cases spraypaint was used to mark every 10 meter intervals. The sections were photographed with an overlap of the pictures for later reconstruction of the entire profile (Appendix 1). The length and strike of the reference line were measured and all fractures, faults and dikes were carefully measured and the following data were measured and described on each fault, 1’st and 2’nd order fracture in the outcrop:

Position (placing) of each fracture were marked as the point where the fracture crossed the reference line. This data was used for reconstructing the profile and calculate fracture-spacing/intensity and trace frequency.

Order/System: The fractures were classified as 1’st, 2’nd or 3’rd order fractures, with the 1’st order fractures as the dominating fractures cross cutting all other fractures (in general > 10 m long in granite outcrops), 2’nd order fractures were less dominating fractures sometimes connecting 1’st order fractures without crossing them (in general between 1 and 4 m), and 3’rd order fractures were minor irregular fractures (in general < 0,5 m). The scale is however relative, and in some cases where the 1’st order fractures may be more than 100 m long, the 2’nd order fractures may be more than 10 m long.
If a clear systematic set of fractures could be recognised in the field it was given a number as system 1 fractures and another set system 2 etc.

Faults were classified according to type (normal/reverse dip-slip faults or transform dextral/sinestral strike slip faults (right hand or left hand movement of the hanging wall). Direction of slickensides were measured and the magnitude of the displacement if possible.

Dikes were described in terms of rock type and thickness and orientation.

Orientation: The orientation of the fracture/fault/dike-contact surface was measured with a compass with a clinometer and the strike and the dip of the plane was measured.

Size: The visible minimum size of the fracture were roughly measured, by measuring the trace-length of the dominating fractures. This can also be done on the reconstructed profiles.

Surface shape: The overall fracture shape (m scale) was described as listric, planar, undulating or irregular.

Surface roughness character: The surface roughness character is described in mm scale as smooth, rough or slickenside (striae).

Remarks: Some fractures/faults had a filling of iron oxide precipitates or quartz crystals, or preferential growth of other crystals on the surface showing the slip direction. The direction of the slickensides were measured on most fault-surfaces. Special types of fractures such as Conjugating shear-fractures, En echelon fracture, plumose jointing etc. were noted if positively identified.

All this data has been carefully analysed primarily in stereographic projections where the different features may be related to different tectonic events.

5. Results

The location of the nine locations are illustrated on figure 5.1. Each site is described and the fracture distribution are presented in the following site description.

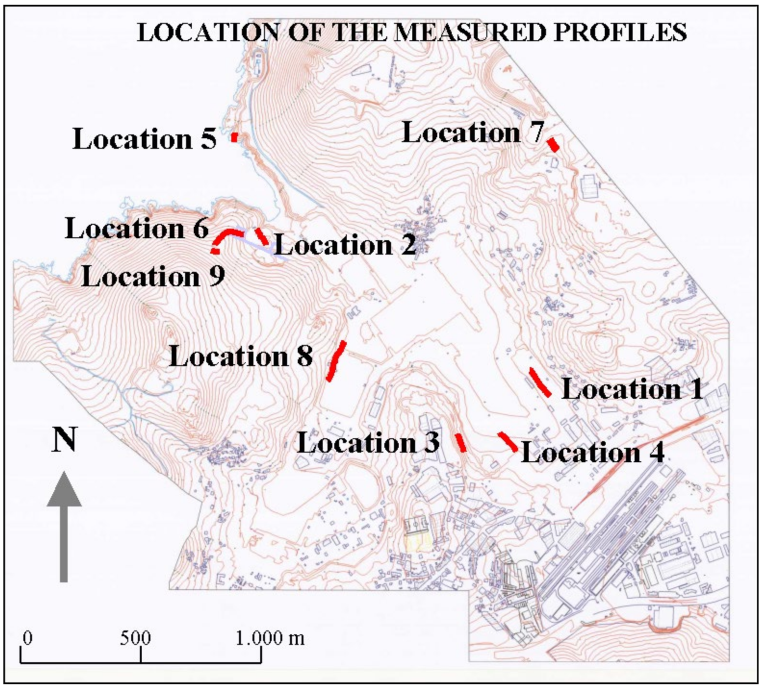

Figure 5.1 The location of the nine sites are marked on the map of the area. The strike of the fractures is likewise illustrated on the Rose diagrams, along with the orientation of large faults which has been visually identified in the area.

5.1 Site description

The description of the different sites refers too the Photo-mosaic and fracture profiles listed in Appendix 1. All the fracture measurements are listed in Appendix 2. The types of outcrops are illustrated on figure 5.2.

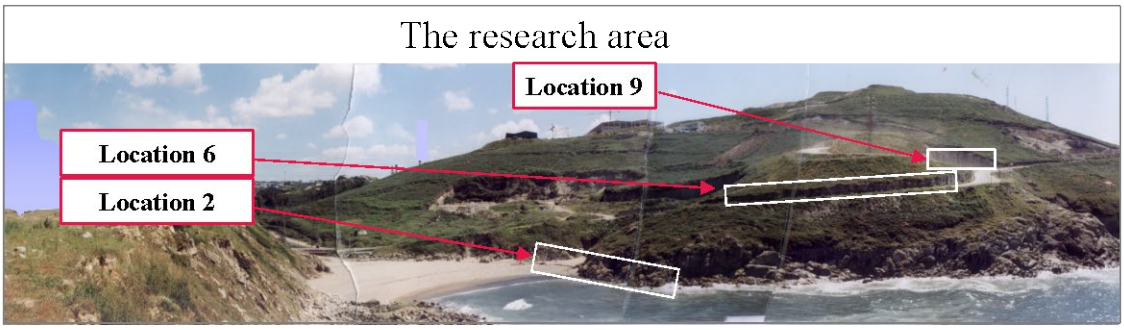

Figure 5.2 View of three locations on the southern hill in the area. The fractures were nicely exposed on the coastal location 2, but the road-cuts on location 6 and 9, were better suited for core sampling and fracture analysis. Location 6 is 180 meter for scale.

Location 1

Profile 1 were measured along a 130 meter long road-cut striking NW-SE see appendix 2.

Description of the profile:
All fractures were measured the first 75 meter, while only 1st order fractures were measured between 75 and 100m on the scan line.
The strike of the profile was 152 degree and a total of 105 1st and 2nd order fractures and 7 faults and were measured along the profile. The profile was excellent exposed, and water seepage was noted on 10 fractures, primarily between 10 and 40 meters.

Fracture density
The fractures has a total fracture intensity close to 3 fractures/m^3(Cumulative spacing 33 cm). The average cumulative spacing of all the 1st order fractures are 54 cm varying from closely spaced fracture zones with a spacing of less than 10 cm to areas of very few fractures with a spacing of several meters.

Fracture distribution
Three clusters with parallel sub-parallel fractures were identified on the stereographic projections (figure 5.3).
System 1 fractures (red figure 5.3) are striking NW-SE with on set dipping steeply towards SW an another set dipping towards NE
System 2 fractures (green figure 5.3) are sub-vertical striking more WNW-ESE. These fractures are sub-parallel to the dike 2 system and they have a general irregular surface character, and may be related to extension during the intrusion of the Leucogranite.
The 3rd fracture system (blue) is primarily located in the first half of the profile. The fractures are striking ESE-WNW and dipping towards SE.
The fracture trace frequency varies from 1,5-1,1 fracture traces/m the first 50 meters and between 80 and 110 m on the profile. it increases to between 2-4 fracture traces/m in two higher fractured zone from 50-80 meter on the profile. The fracture distribution along the profile varies thus greatly, and the distribution of fractures are generally heterogeneous, with areas of less fractured granite in between zones of higher fracture density. The orientation of the fractures also varies along the profile.

Event stratigraphy
The order of tectonic events are difficult as the dikes and faults are not truncating each other, but the following order of events were deduced from the observations:

1. Intrusion of Granodiorite
2. Intrusion of dike 1 (60^0/40SE)
3. Strike slip faults ?
4. Intrusion of dike 2 (85-110^0/40-90N) maybe associated with System 2 fractures.

Normal faults ?

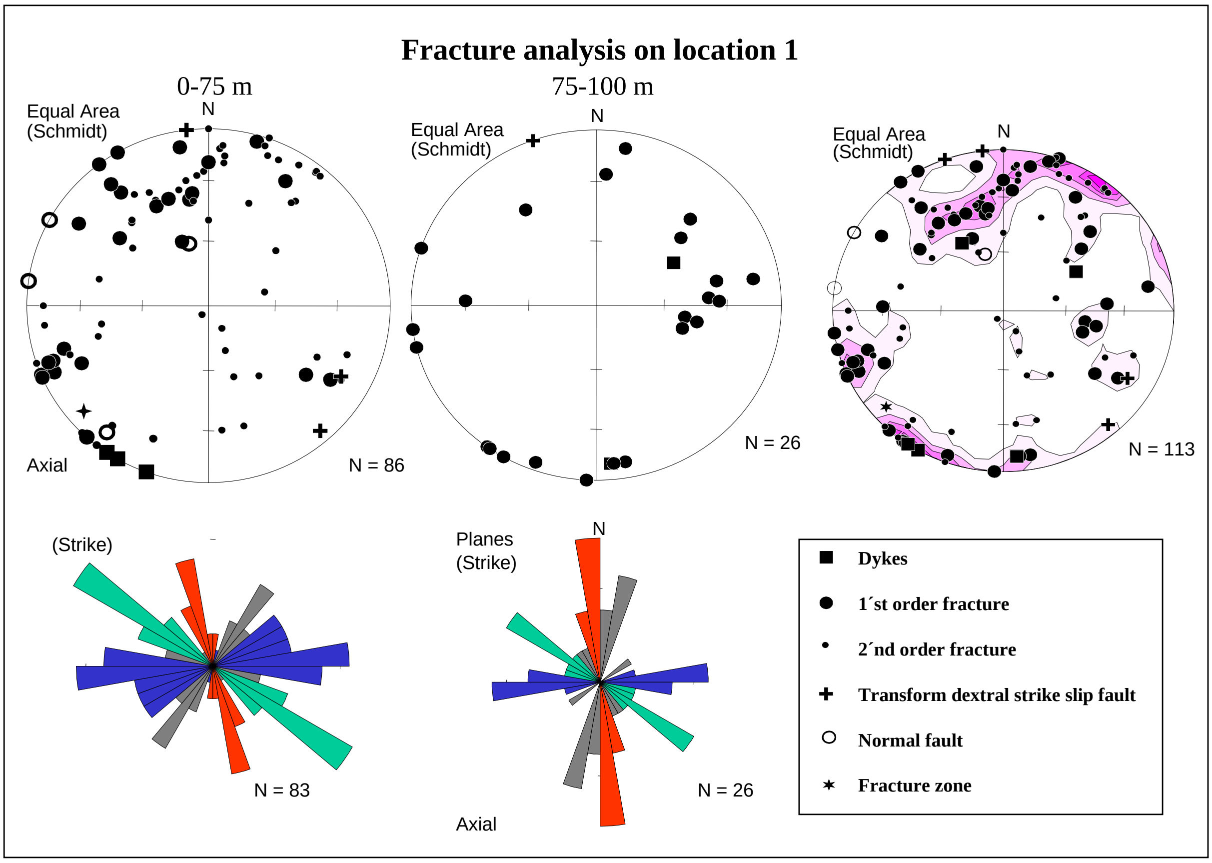

Figure 5.3. Fracture analysis on location 1. The orientation of fractures are marked on stereographic projections and the strike is illustrated on rose diagrams. Fractures that are considered connected to the same tectonic event has been marked in different colours.

Location 2

Profile 2 were measured along a 30 meter long well exposed granite outcrops along the coast just south of the sand beach (see figure 5.2).

Description of the profile:
The profile had a rather rough morphology, but erosion from the sea clearly marked important structures, thus enabled the identification of large fracture zones and other structures. The profile was not well suited for construction of photo mosaics and the profile has accordingly not been included in appendix 1.The strike of the profile was roughly 165 degree and a total of 23 1st and 29 2nd order fractures and 1 fault were measured along the profile. An important feature was the occurrences of large quartz crystals in many fractures and faults.

Fracture density
The fractures has a total fracture intensity close to 2,5 fractures/m^3 (Cumulative spacing 40 cm). The average cumulative spacing of all the 1st order fractures are 1,18 m and 66 cm for the 2nd order fractures. The total fracture trace frequency is 1,45 fracture 1st and 2nd order fracture traces pr m.

Fracture distribution

Three clusters with parallel sub-parallel fractures were identified on the stereographic projections (figure 5.4). The dominating fractures are striking almost E-W. Transform strike slip fractures with displacement of 30-40 cm truncate a leucogranite dike in the southern part of the profile. The fault have later been reactivated and has opened 1-2 cm. Quartz crystals has precipitated inside the fault and in some of the major fractures. Lack of preferential growth in most of the fractures/faults indicate a pure opening mode without strike-slip displacement between the two walls. This indicates tensile stress in a north south direction. The following fracture systems were identified.

System 1 fractures (blue figure 5.4) are striking NE-SW. They are generally secondary fractures with an undulating rough surface.

System 2 fractures (red figure 5.4) are sub-vertical secondary fractures striking more NW-SE.

System 3 fractures (green) The fractures are sub-vertical striking ENE-WSW. These fractures forms the dominating fractures on this location.

Event stratigraphy

The geological events took place in the following order on location 2.

1. Intrusion of Granodiorite
2. Intrusion of dike (16^0/45SE)
3. Dextral strike slip faulting 85-100^0/90.
4. Extension: Reactivation and opening of faults and fractures. Crystallisation of quartz inside the fractures.

Fracture analysis on location 2

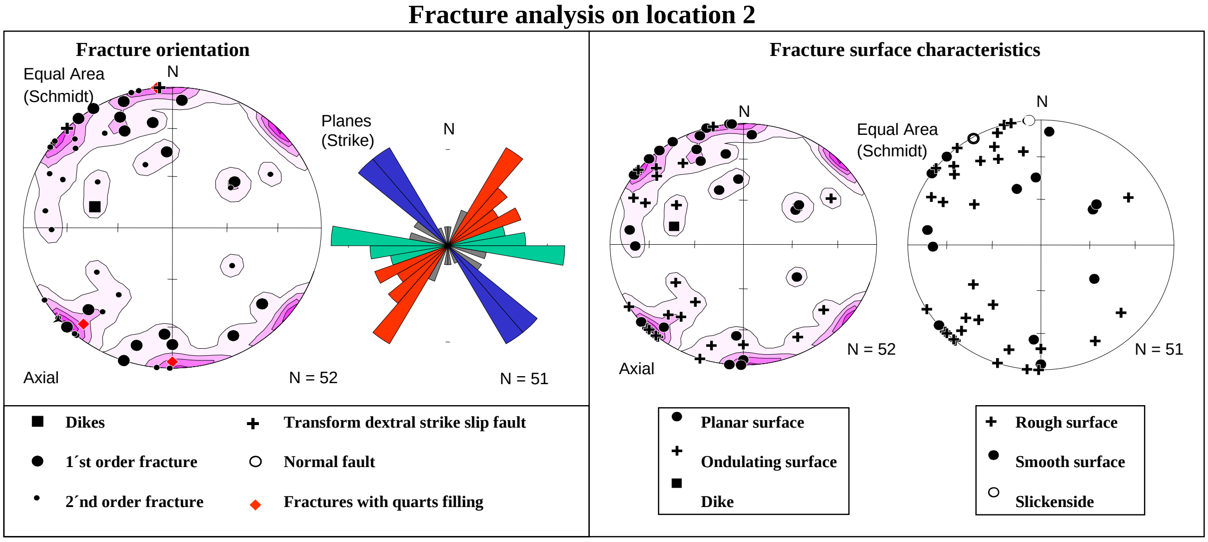

Figure 5.4 Fracture distribution on location 2. Three cluster of fractures were identified, with the green cluster representing the dominating fractures on this site.

Location 3

Profile 3 were measured along a 40 meter long road-cut striking NW-SE see appendix 2.

Description of the profile:

The strike of the profile was 160^0 and a total of 62 1st and 2nd order fractures were measured along the profile. The profile was partly covered with loose material. An almost five meter wide intrusion of leucogranite (60^0/90) has intruded the granodiorite between 8 and 13 meter, see profile 3 (appendix 1).

Fracture density

The fractures has a total fracture intensity of 2.4 fractures/m^3 (Cumulative spacing 41 cm). The average cumulative spacing of all the 1st order fractures are 1,18 m cm varying from more closely spaced fracture in the first 20 meters to areas of very few fractures with a spacing of several meters after 20 meter. The dyke is remarkable closely spaced (10-7 cm) by secondary fractures.

Fracture distribution

Three clusters with parallel sub-parallel fractures were identified on the stereographic projections (figure 5.5).

System 1 fractures (blue figure 5.4) are striking NE-SW. These fractures are dominating the profile between 0 and 15 meter and are striking parallel to the dike. The fractures sometimes forms a zone with 3-7 fractures closely spaced (~15cm).
System 2 fractures (red) are restricted to the Leucogranite and does not penetrate the granodiorite. They are related to stress release during cooling, and forms a system of two conjugating fracture sets with the orientations ~145/85 NE and ~5/70W.
System 3 fractures (green) are sub-vertical fractures striking almost E-W. These fractures are truncating all other fractures including the dike and are accordingly considered youngest.

Event stratigraphy

The following order of events were deduced from the observations:

1. Intrusion of Granodiorite
2. Intrusion of dike (60^0/90SE) parallel to system 1 fractures (blue). Same event or later.
3. System 2 fractures (red) inside dike.
4. System 3 fractures (green) penetrate dike.

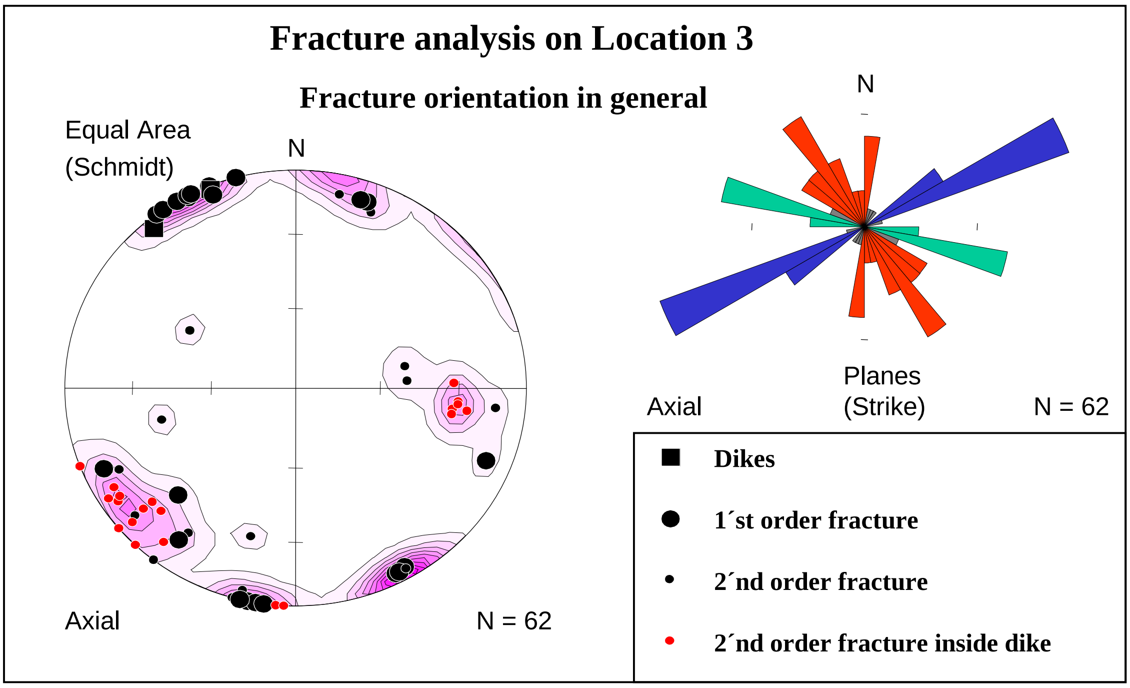

Figure 5.5. The distribution of fractures and the three systems marked with different colours.

Location 4

Profile 4 were measured along a 36 meter long road-cut striking NW-SE.

Description of the profile:
The strike of the profile was 148^0 and a total of 47 1st and 2nd order fractures were measured along the profile. The profile was poorly exposed and partly covered with loose material. The profile is situated a few hundred meters from profile 3.

Fracture density
The fractures has a total fracture intensity of 2.92 fractures/m^3 (Cumulative spacing 34 cm). The average cumulative spacing of all the 1st order fractures is 1,29 m, while it is 50 cm for the 2nd order fractures. The trace frequency is 2,02 fracture traces/m.

Fracture distribution
Three clusters with parallel sub-parallel fractures were identified on the stereographic projections (figure 5.6).

System 1 fractures (blue figure 5.6) are striking NE-SW. These fractures are the dominating 1st order fractures in the profile.
System 2 fractures (red) consists of a secondary fracture system striking NW-SE.
System 3 fractures (green) are sub-vertical fractures striking almost E-W. These fractures consists mainly of 2nd order fractures.

Event stratigraphy

The following order of events were deduced from the observations:

1. Intrusion of Granodiorite
2. Fracturing. Lack of intrusions and faults prevent determination of the order of fracturing.

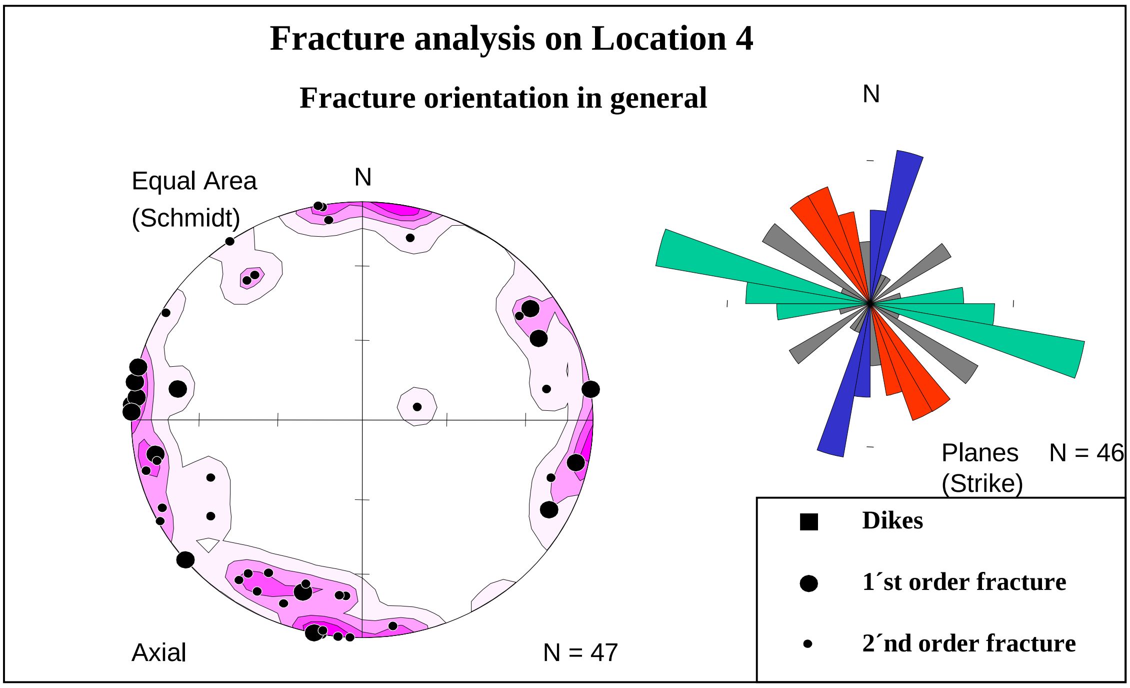

Figure 5.6 Distribution of fractures on location 4.

Location 5

Location 5 were located on granite outcrops on the coastal cliffs approximately 500 meters north of the beach (Figure 5.1). This is a key locality in order to understand the geological history of the area. The contact between leucogranite and granodiorite is well exposed on this location. The contact strike ~35^0 and dip 40-45^0NW.

The leucogranite is light brown with a large content of mica (muscovite), quartz and feldspar. Some dark minerals gives the leucogranite a foliated appearance (30-34^0/6-12^0NW) on this site, while it is rather massive on other sites.

The Granodiorite coarse-grained with large quartz crystals and rohmb shaped feldspar crystals up to 2-3 cm long. The granodiorite is intensively truncated by dikes and larger bodies of leucogranite. It is strongly deformed after the intrusion, and just north-west of the site appears a large contact towards the Pre-Cambrian meta-sediments, that consists of conglomerates intruded by a dark fine-grained rock, probably amfibolite. The contact strikes NE-SW and striations on the surface indicate the presence of a large thrust in the contact between the Pre-Cambrian rocks and the granite. This is documented on the geological map of the area (figure 1.1).

The leucogranite intrusions striking 40-50^0/90 has been intruded into the granodiorite. They have later on been truncated by a large system of small reverse faults. The fault-planes are often sealed with large quartz crystals, and preferential growth of some of the crystals shows a very distinct movement direction of the hanging wall from SW towards NE (60^0). This direction coincide with the dextral faults measured elsewhere in the area (location 6-7-9). Several fracture directions dominate on this location.

The leucogranite are clearly more intensive fractured (~120/80NE) than the granodiorite. A very large (>200m) fracture (26^0/72 NW) are penetrating the whole area. It is parallel to two other major fractures further south and it is also parallel to the thrust fault that forms the contact towards the older rocks north-west of the area, and may thus be related to the same tectonic event. It has been intruded by leucogranite and may accordingly be older or the same age, thus indicating the thrusting to take place, at the same time as the widespread dextral strike slip faulting striking 80-100^0 on other locations.

Event stratigraphy

The following order of events were deduced from the observations on location 5:

1. Intrusion of Granodiorite into Pre-Cambrian meta-sediments.
2. Large scale thrust faulting of Pre-Cambrian meta-sediments onto the Granodiorite intrusion. Maybe associated with formation of major fractures (>200m) striking 25-35^0 dipping towards NW, and dextral strike slip faulting striking 80-100^0.
3. Intrusion of leucogranite.
4. Reverse faulting + strike slip faults striking ~60^0.
5. New fracture system striking 26-18^0.

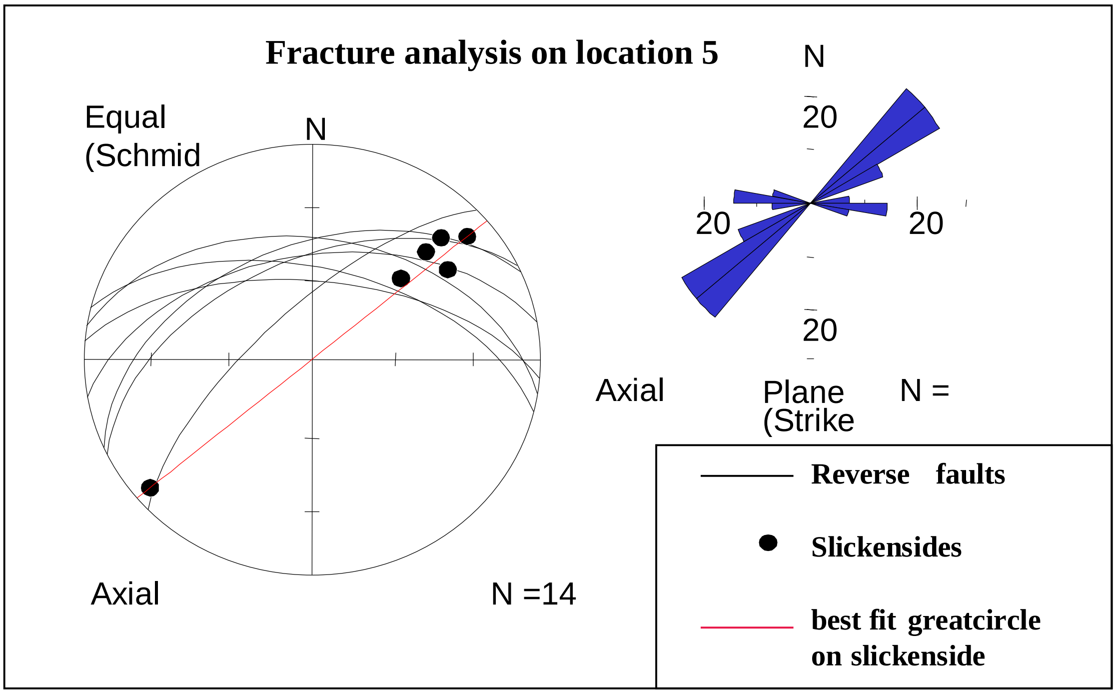

Figure 5.7 shows orientation of reverse faults and slickensides measured on faults surfaces. These faults truncate the leucogranite intrusions and are accordingly younger. NE-SW striking fractures truncate the faults and are thus the youngest structures on this site.

Location 6

Profile 6 was measured along a 180 m long road-cut. 60 m of the profile was carefully measured. The profile was the longest of the measured profiles, it was excellent exposed, and easily accessible, and the location was therefore selected for the core sampling of impregnated fractures. All the sites that were selected for core sampling are marked on profile 6 (appendix 1).

Description of the profile:
The road was turning from an SE-NW direction towards a NE-SW direction along the distance and the profile changed strike accordingly. The measured section was striking approximately 100^0. A total of 68 1^{st} and 2^{nd} order fractures and faults were measured along 60 meter of the profile.

Fracture density
The fractures and faults have a total intensity of 2,15 fractures/m^3 (Cumulative spacing 47 cm). The average cumulative spacing of all the 1^{st} order fractures is 72 cm, while it is 140 cm for the 2^{nd} order fractures. The trace frequency is 1,0 fracture traces/m. The most impressive feature is a regular zone of strike slip faults that dominates the western part of the profile. The faults are closely spaced in a 30-40 m wide zone (50-100 cm) and probably km long.

Fracture distribution
Three clusters with parallel sub-parallel fractures/faults were identified on the stereographic projections (figure 5.8).

System 1 fractures (blue, figure 5.8) consist of sub-vertical dextral strike slip transform faults and major planar smooth fractures striking ENE-WSW 60-90^0. The faults are typically displaced 30-40 cm with a clear slickenside on the surface. Some of the faults have been intruded by leucogranite.
System 2 fractures (red) consist of a system of undulating/irregular fractures with a rough surface striking NNE-SSE (10-30^0).
System 3 fractures (green) are sub-vertical generally undulating rough fractures and normal faults striking almost E-W dipping ~60^0 towards north. Some dikes and all strike slip faults are truncated by the normal faults.

Event stratigraphy
The following order of events were deduced from the observations:
1. Intrusion of granodiorite.
2. System 1 fractures and dextral strike slip faults
3. Intrusion of thin dikes with leucogranite.
4. Normal faulting and intrusions of large (>1m thick) irregular dikes during extensional stress regime.

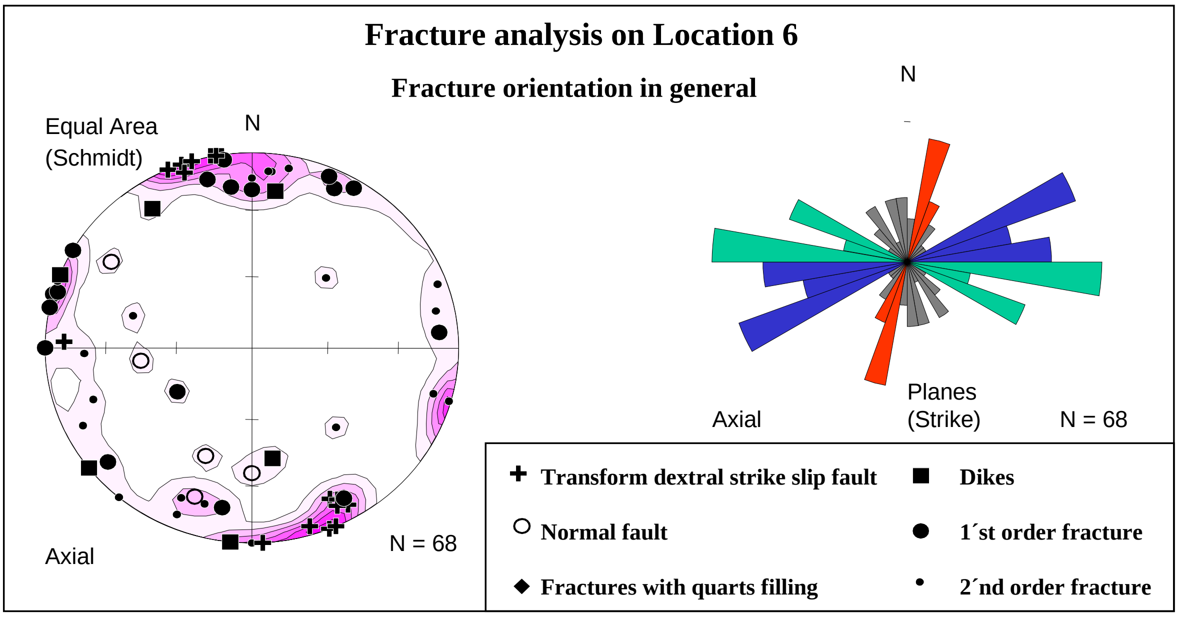

Figure 5.8 Fracture and fault orientation on location 6.

Location 7

Profile 7 was measured in a freshly excavated area on the northern hill (figure 5.1). Outcrop had a half-moon shape and approximately 50 m of profile was measured. The fractures were perfectly exposed, and the presence of en echelon fractures, and two clearly different intrusive events, combined with both strike slip and normal faulting, facilitated a detailed analysis of tectonic history of this location.

Description of the profile:

The measured section was striking approximately N-S turning towards NE-SW. A total of 66 1st and 2nd order fractures and faults were measured along 50 m of the profile.

Fracture density

The fractures and faults have a total intensity of 1,45 fractures/m^3 (Cumulative spacing 69 cm). The average cumulative spacing of all the 1st order fractures is 104 cm, while it is 221 cm for the 2nd order fractures. The trace frequency is 1,32 fracture traces/m. The most impressive features are a, more than 20 m wide zone of dextral strike slip faults, with an average spacing of 1,5 meter, that dominates the northern part of the profile.

Fracture distribution

Four systems of related fractures/faults were identified on the stereographic projections (figure 5.9).

System 1 fractures (purple, figure 5.9) are dikes with completely sealed coarse grained crystals striking NE-SW dipping 60-70^{0}NW. These are regarded to be quite old and they are truncated by transform faults and younger leucogranite dikes.

System 2 fractures (red) consist of sub-vertical dextral strike-slip transform faults and major planar smooth fractures striking ENE-WSW 70-90^0. The faults are typically displaced 30-40 cm with a clear slickenside on the surface.
System 3 fractures (green) are sub-vertical fractures and normal faults striking 90-120^0 dipping 90-60^0 NNW. Dikes and all strike slip faults are truncated by the normal faults. One very large fracture (138/80SW) has opened almost 20 cm. Syntaxial growth of quartz crystals shows that no displacement took place during the opening and the fracture is related to the system 3 extensional fractures.
System 4 fractures (blue) are large (>50m) curved irregular sub-horizontal fractures with a spacing of > 1m decreasing towards the surface.

Event stratigraphy

The following order of events were deduced from the observations. The formation of en echelon fractures in relation with the strike slip faults, enable the construction of the stress field at the time of deformation. See figure 5.9. The order of events are as follows:

1. Granodiorite intrusion.
2. Intrusion of coarse grained dike (50-25^0./60-70 NW (NW-SE extension)
3. Strike slip dextral faulting (striking 70-90^0) and en echelon fractures striking 100-120^0. (lateral compression NW-SE)
4. Intrusion of leucogranite (striking 100-106^0) and normal faulting (striking 90-110^0, dipping 80-60^{0}NE) (NE-SW extension).
5. Sub-horizontal dome shaped sheet fractures, probably formed as a result of stress release and contraction during uplift and cooling.

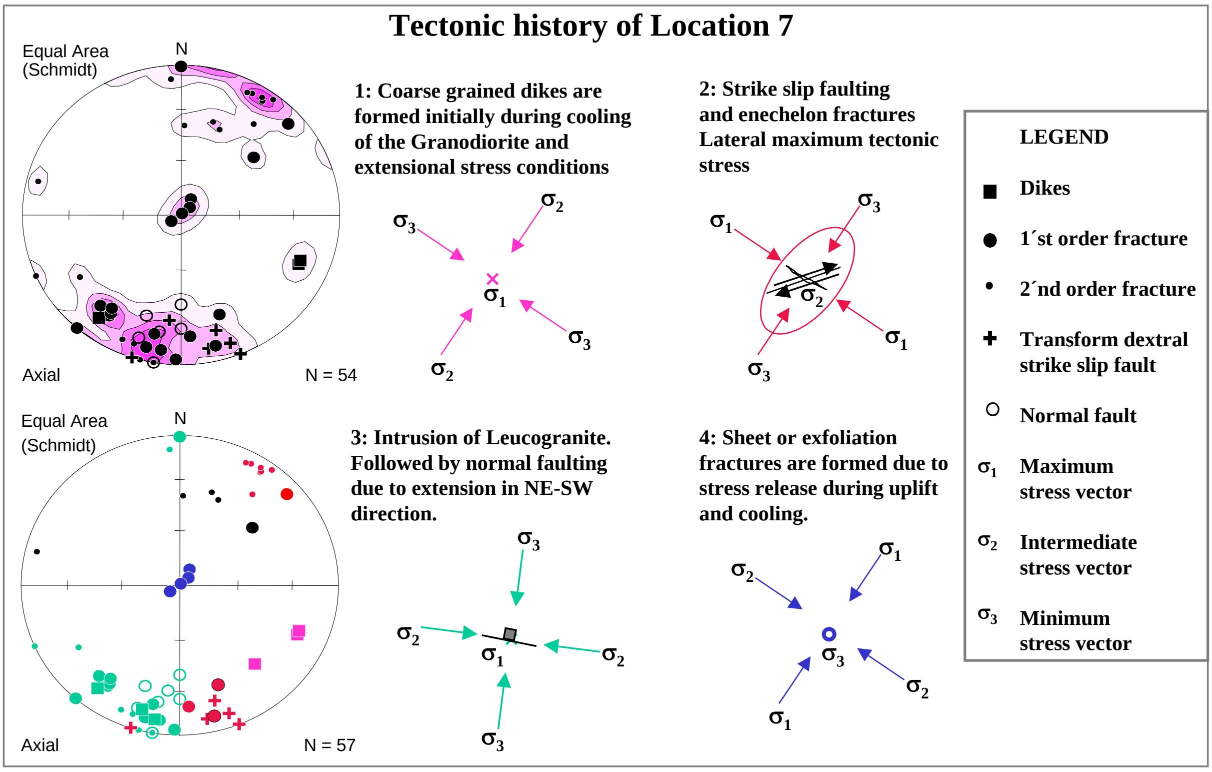

Figure 5.9 Stress history combined with the classification of fractures and fault systems on location 7.

Location 8

Profile 8 was measured along a 80 meter long road-cut in the south-western part of the area. The profile was excellent exposed (appendix 1).

Description of the profile:

The measured section was striking approximately 35^0. A total of 97 1^{st} and 2^{nd} order fractures and faults were measured along 60 meter of the profile.

Fracture density

The fractures and faults have a total intensity of 2,80 fractures/m^3 (Cumulative spacing 34 cm). The average cumulative spacing of all the 1^{st} order fractures are 69 cm, while it is 74 cm for the 2^{nd} order fractures. The average trace frequency for 1^{st} and 2^{nd} order fractures are 1,62 fracture traces/m. The trace frequency for all fractures varies from more than 3 fracture traces/m in the start of the profile to less than 1,5 in the central part of the profile and then it rises to more than 3 fracture traces/m in the end of the profile.

Fracture distribution

Three clusters with parallel sub-parallel fractures/faults were identified on the stereographic projections (figure 5.10).

System 1 fractures (blue, figure 5.10) consist of two set of fractures striking 30-60^0/60 NW and SE.

System 2 fractures (red) consist of a system of undulating sub-vertical fractures with a rough surface, striking SE-NW.

System. 3 fractures (green) are sub-vertical fractures, normal and strike slip faults striking 90-150^0 with a steep dip (75-90^0) towards NE. Some vertical irregular leucogranite dikes are striking E-W. They are truncated by the normal faults.

Most of the faults are associated with highly fractured zones and clearly conduct water. 6 out of 7 faults are thus leaking water on this location.

Event stratigraphy

The following order of events were deduced from the observations:

1. Intrusion of granodiorite.
2. Dextral strike slip faulting?
3. Intrusion of thin dikes with leucogranite.
4. Normal faulting during.

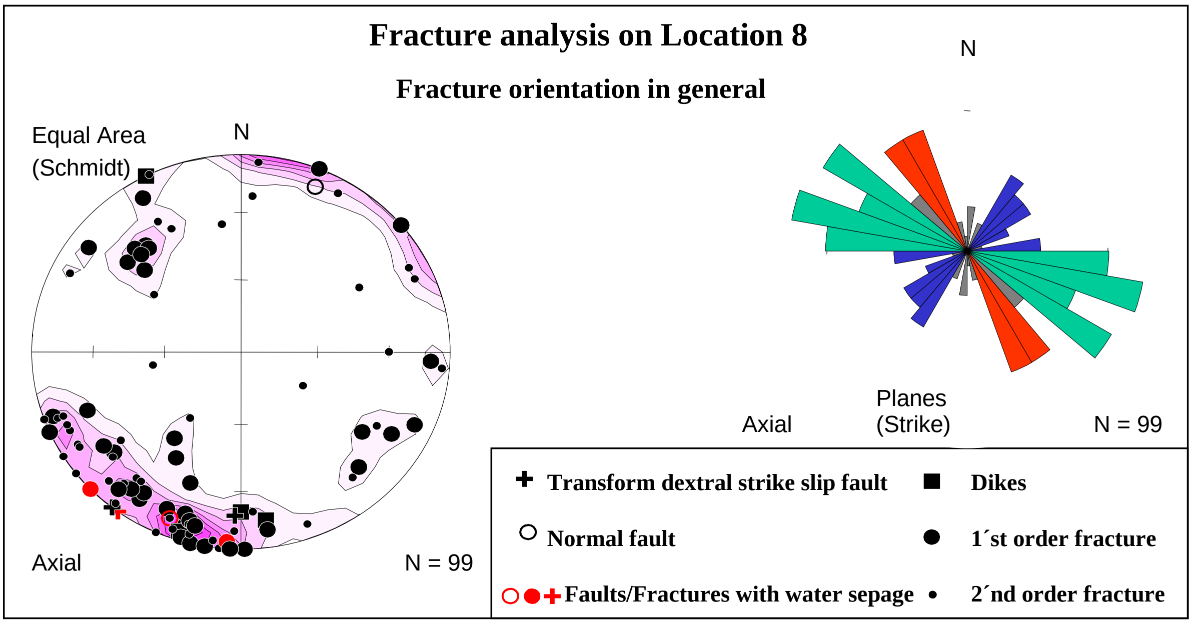

Figure 5.10. Fracture fault distribution on location 8. Structures conducting water seepage are marked with red.

Location 9

Profile 9 was measured perpendicular to the strike of the dextral transform fault-zone that was described on location 6. Profile 9 is thus situated less than 100 m from location 6 and represents the highest fracture/fault density in the area (see appendix 1, profile 9).

Description of the profile:

The profile is a fresh roadcut approximately 50 m long and more than 10 m high. The measured section was striking approximately 100^0. A total of 62 1^{st} and 2^{nd} order fractures and faults were measured along 30 m of the profile.

Fracture density

The fractures and faults have a total intensity of 4,64 fractures/m^3 (Cumulative spacing is 21 cm). The average cumulative spacing of all the 1^{st} order fracture/faults is 33 cm, while it is 61 cm for the 2^{nd} order fractures. The trace frequency is 2,13 fracture traces/m. The most impressive features are a regular zone of strike slip faults that dominate the western part of the profile. The faults are closely spaced in a 30-40 m wide zone (50-100 cm spacing) and probably extends several km. This is the highest fracture/fault density measured on the Spanish site and the granodiorite is highly weathered in the western end of the profile. The deeply weathered granite is regarded to be associated with this type of fault-one in most locations.

Fracture distribution

Three clusters with parallel sub-parallel fractures/faults were identified on the stereographic projections (figure 5.11).

System 1 fractures (blue, figure 5.11) consist of sub-vertical dextral strike-slip transform faults and major planar smooth fractures striking ENE-WSW 60-90^0. The faults are typically displaced 30-40 cm with a clear slickenside on the surface. Some of the faults has been intruded by leucogranite. The leucogranite tends to follow the faults, but truncate several faults in the central part of the profile (see profile 9).

System 2 fractures (red) consist of a system of weakly developed secondary undulating/irregular sub-vertical fractures with a rough surface striking NW-SE.

System 3 fractures (green) are sub-vertical generally undulating rough fractures and normal faults striking almost E-W dipping ~50^0 towards north. All strike slip faults are truncated by the normal faults.

Event stratigraphy

The following order of events were deduced from the observations:

1. Intrusion of granodiorite.
2. System 1 fractures and dextral strike slip faults
3. Intrusion of dikes with leucogranite.
4. Normal faulting.
5.

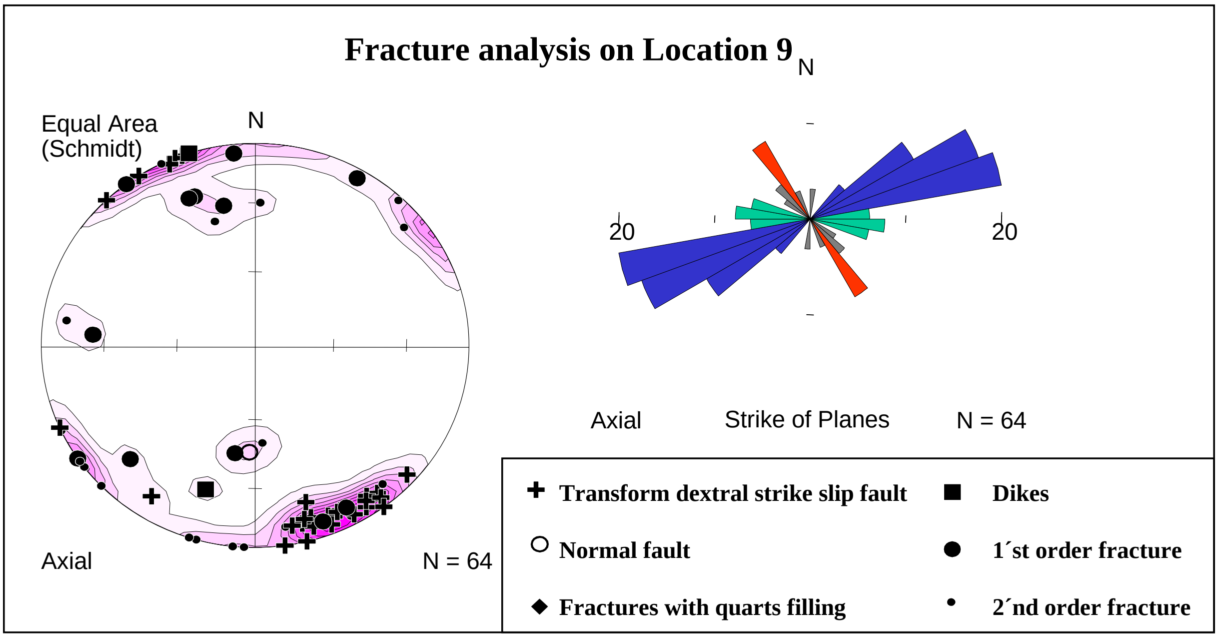

Figure 5.11 Distribution of fractures and faults on location 9.

6 Fracture distribution model

Based on the observations and literature data, a tectonic model, as well as a fracture distribution model, has been constructed. This model includes results concerning:

1. Spatial distribution of the fractures.
2. Quantitative fracture properties such as: Fracture density, fracture distribution (orientation), fracture classification into typical fracture types with characteristic surface characteristics (aperture). This data is based on field measurements and construction of the outcrop maps (appendix 1)
3. Fracture surface characterisation.
4. Distribution of fracture zones, weathered granite and fresh granite on a larger scale.
5. Tectonic history of the fractures/faults are correlated to the regional history of the area.

6.1 Spatial distribution of fractures

Figure 6.1 shows the regional orientation of all the measured 1st and 2nd order fractures, faults, dikes and slickensides. All orientation data are listed in appendix 2.

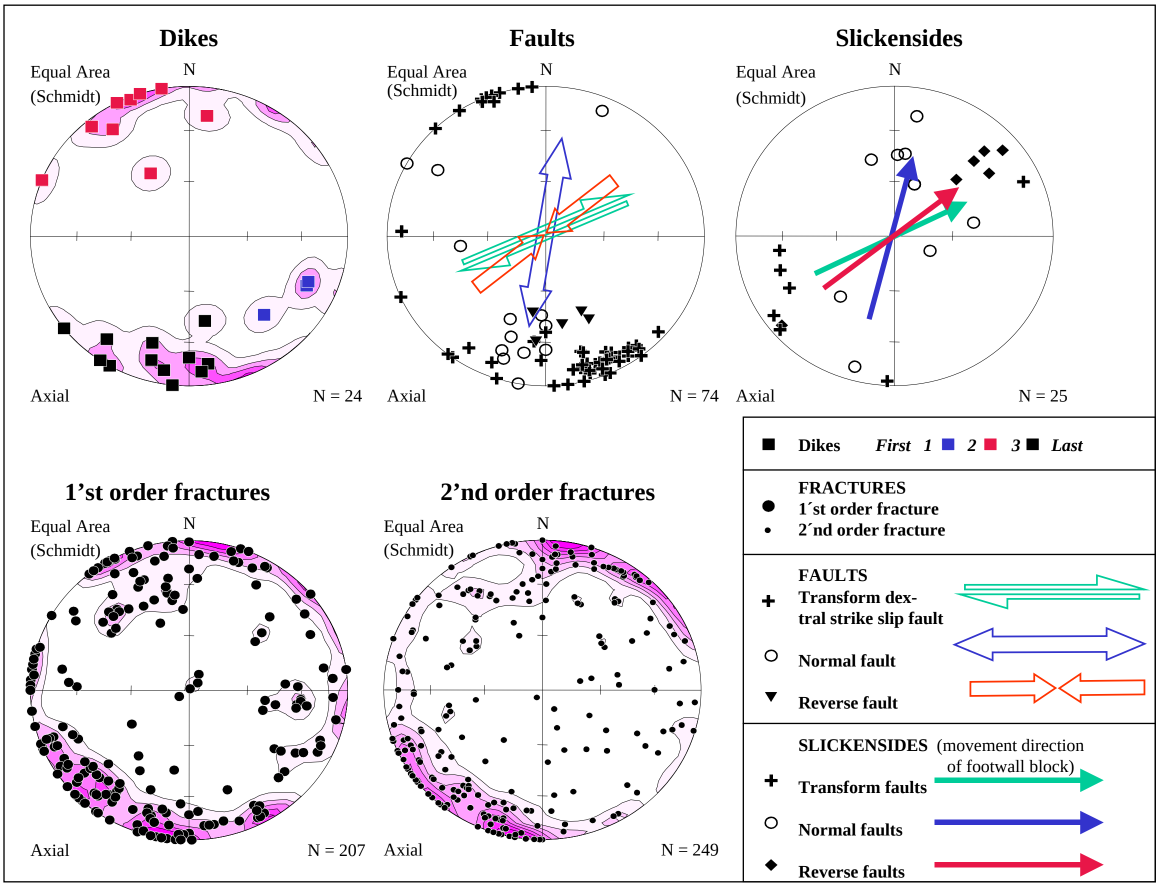

Figure 6.1 Distribution of fractures, faults, dikes and slickensides (on fault-planes) on all locations.

The results show that the different systems of dikes and faults are systematically oriented in different areas. They may thus be related to regional stress fields and regional tectonic events while fractures especially 2nd order fractures are more randomly oriented and may be related to more heterogeneous local stress fields. The 1st order fractures are generally striking ESE-WNW, with an overall steep dip. The 2nd order fractures shows the same dominant direction but also a large group of randomly distributed fractures. Three different clusters of dikes have been identified. The oldest dikes (blue, on figure 6.1) are truncated by younger red and black dikes. The red dikes have sometimes intruded dextral strike slip faults, which orientation then controls the dike orientation, even though the dike belongs to the black system.

The fracture strike diagrams illustrated on figure 6.2 show a domination of dextral strike slip fault zones striking ENE-WSW in the western part of the area. The fracture orientation seems rather non-systematic but dominant extensional fractures and normal faults striking ESE-WNW are quite abundant on all locations.

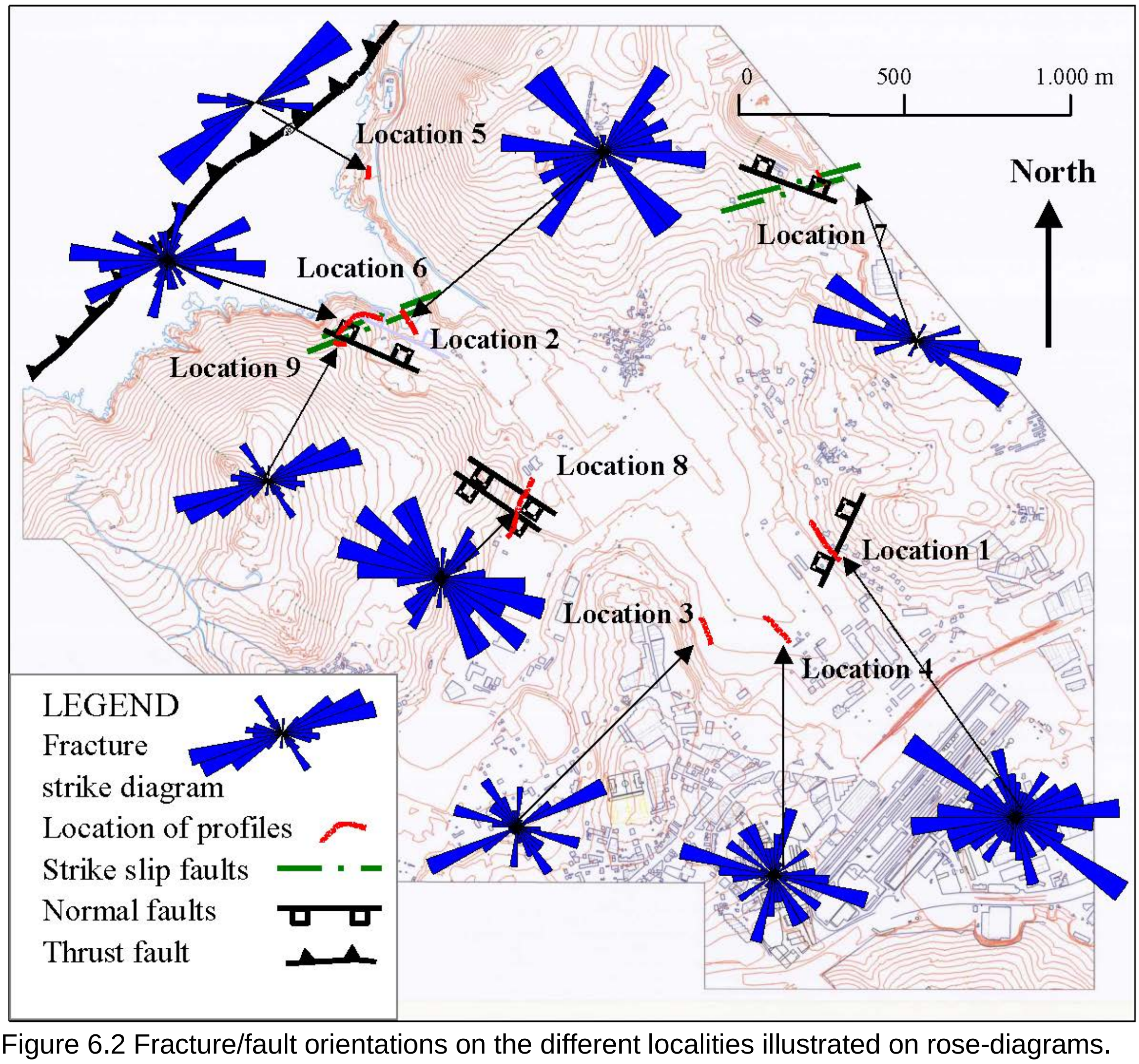

Figure 6.2 Fracture/fault orientations on the different localities illustrated on rose-diagrams.

6.2 Quantitative fracture properties

The average spacing and intensity of the fractures has been calculated for all the individual locations, and the trace frequency has been measured in order to describe the density variation.

Fracture Intensity and Spacing.

The fracture density properties of the fractures are listed in table 6.1. The first three columns shows the number of fractures included in the calculation of the fracture properties.

FRACTURE PROPERTIES											
	Number of fractures			Cum. Fracture Spacing (m)			Fracture Intensity (frac/m)			Trace Frequency	
	N 1'st	N 2'nd	N tot	S 1'st m	S 2'nd m	Sp. Tot.	I_1 Fr./m	I_2 Fr./m	I_{tot}	F_{trace}	$I_{tot/}F_{trace}$
Location 1	47	56	103	0,54	0,88	0,33	1,85	1,14	2,99	1,15	1,65
Location 2	23	29	52	1,18	0,66	0,40	0,84	1,51	2,51	1,73	1,45
Location 3	27	19	46	0,78	0,89	0,41	1,28	1,12	2,44	1,53	1,59
Location 4	15	37	52	1,29	0,50	0,34	0,77	2,00	2,92	1,44	2,02
Location 6	38	22	60	0,72	1,40	0,47	1,38	0,71	2,15	1,00	2,15
Location 7	44	22	66	1,04	2,21	0,69	0,96	0,45	1,45	1,32	1,10
Location 8	45	52	97	0,69	0,74	0,34	1,45	1,35	2,80	1,62	1,82
Location 9	41	21	62	0,33	0,61	0,21	3,01	1,64	4,65	2,13	2,27

Table 6.1 Fracture/fault spacing, intensity and trace frequency values on all the locations (for definition of the fracture properties see figure 4.1)..

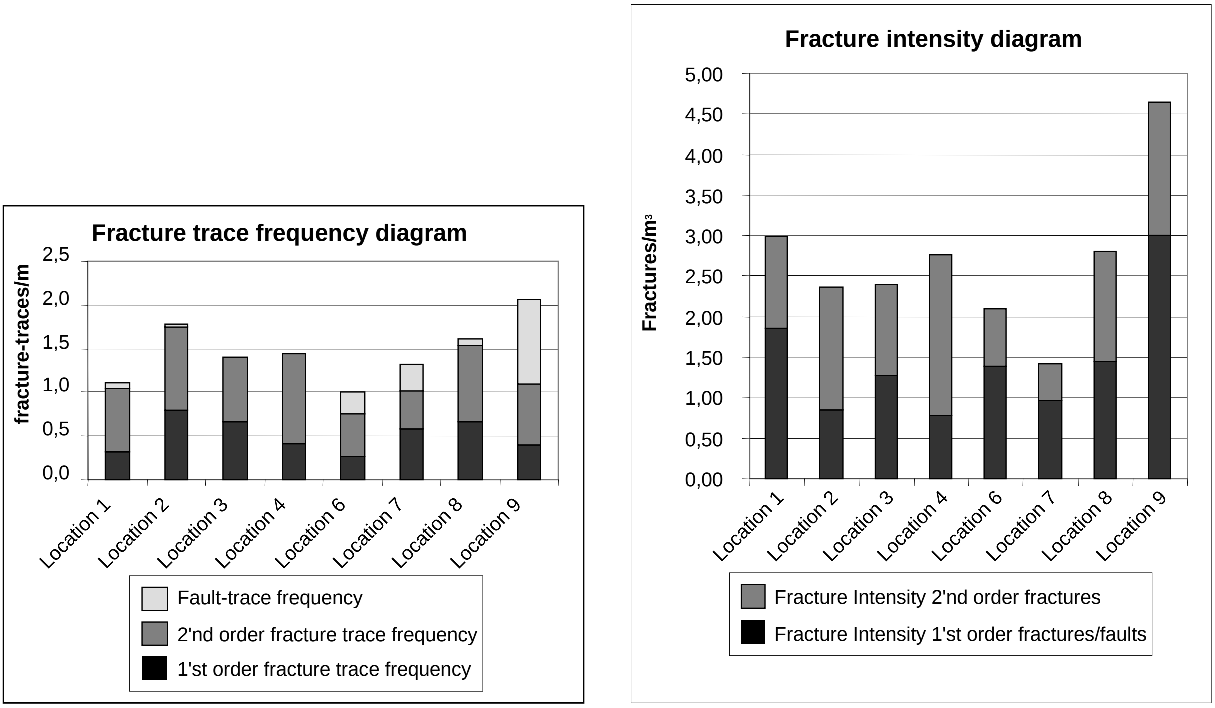

Figure 6.3 Fracture trace frequency and fracture intensity variation on the 9 locations.

The cumulative spacing and intensity of the 1st order fractures/faults and 2nd order fractures are illustrated in the next three columns, while the fracture trace frequency and the Intensity/frequency ratio are calculated in the last two columns. This value shows how biased the trace frequency value are. The calculation of the fracture Intensity in 10 degree intervals are listed in Appendix 3. The fracture intensity and trace frequency of 1st and 2nd order fractures are illustrated in figure 6.3.

Fracture trace frequency variation along the profiles.

The fracture trace frequency variation of all the fractures along profile 1, 3, 6, 8, and 9 was counted from the profiles in appendix 1. This illustrates the fracture density variation in 10 m intervals along the profiles. The results are illustrated in figure 6.4. It shows clearly that the variation within one profile varies more than 100% between zones of low density and highly fractured areas.

The fracture trace frequency data are generally biased due to the orientation of the fractures. Fracture systems, that truncates the profile at a small angle, will always be underrepresented and fractures parallel to the profile will not be included at all. The ratio between the fracture intensity and the trace frequency (table 6.1) illustrates how biased the data are and facilitates an opportunity to correlate the data in figure 6.4. The fracture zones have in general trace frequency values between 3 and 4,5 fracture traces pr/m while the average fractured granite has values close to 2 fracture traces/m.

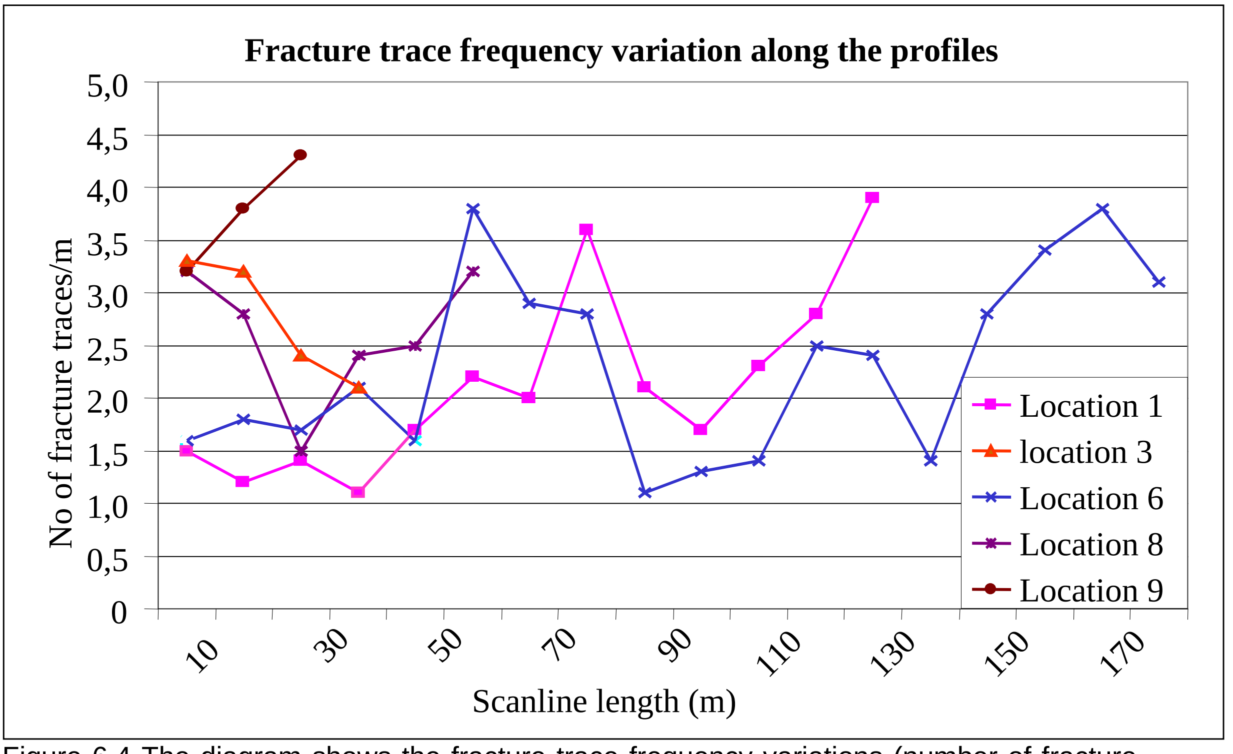

Figure 6.4 The diagram shows the fracture trace frequency variations (number of fracture traces pr/ for 1st 2nd and 3rd order fractures in 10 meter intervals along profile 1, 3, 4, 6, 8 and 9.

The ratio between the fracture intensity and the trace frequency is illustrated on figure 6.5 and in general the trace frequency is between 1,1 and 2,3 times smaller than the true fracture intensity. The average ratio on this location is 1,76.

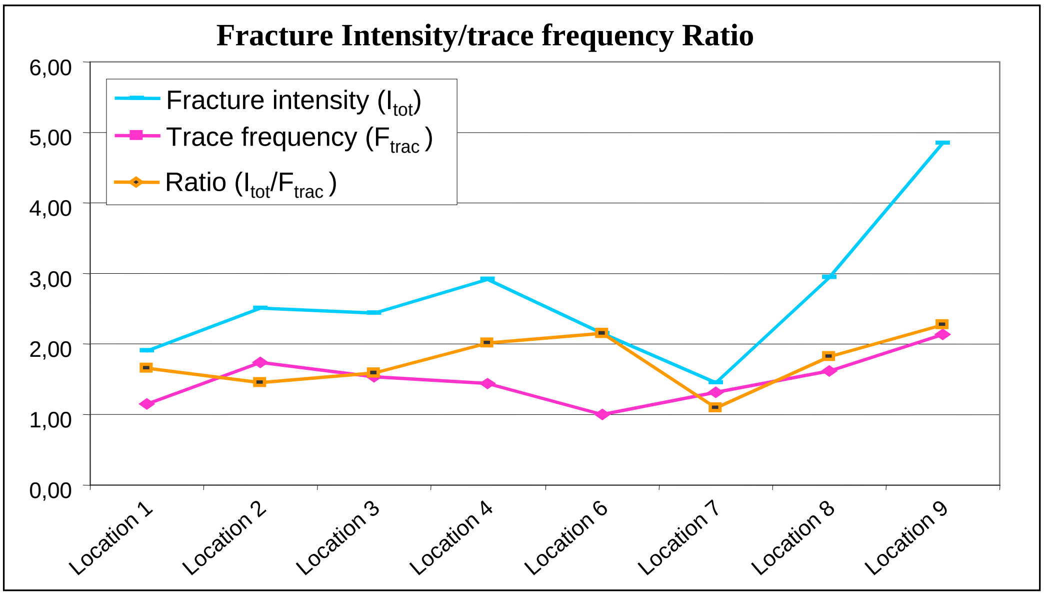

Figure 6.5 Ratio between fracture Intensity and fracture trace frequency.

6.3 Fracture surface characterisation.

The fracture/fault surface characteristics were described on 365 fractures/faults and as demonstrated on figure 6.6 the faults showed a clear dominance of planar surfaces with a smooth striated surface (slickensides). The dominant 1st order fractures striking 90-120^0 are generally planar/undulating with a smooth fracture surface. The majority of these fractures are sub-parallel to the faults in the area and are thus classified as shear fractures that typically develop a more planar shape than tensile fractures.

Fracture surface characters					
Surface shape (m scale)			Surface roughness (mm scale)		
Irregular	31	8,5%	Rough	196	54,9%
Undulating	183	50,1%	Smooth	111	31,1%
Planar	151	41,4%	Slickenside	50	14,0%

Table 6.2 Number of fractures/faults with different surface characteristics.

The undulating/irregular fractures usually have a rough surface. These fractures are mostly represented by 2nd order fractures, but also 1st order fractures with a rough surface are abundant. These fractures are regarded to have a dominating extensional origin, but several fractures have been reactivated during later tectonic events. This has been documented by preferential growth of quartz crystal, perpendicular to the fault surface, during tensile opening mode of former faults at location 2, 5 and 7.

The surface characteristics were used as one criterion for sampling representative fractures for detailed aperture analysis (Rosenbom et al 2001)

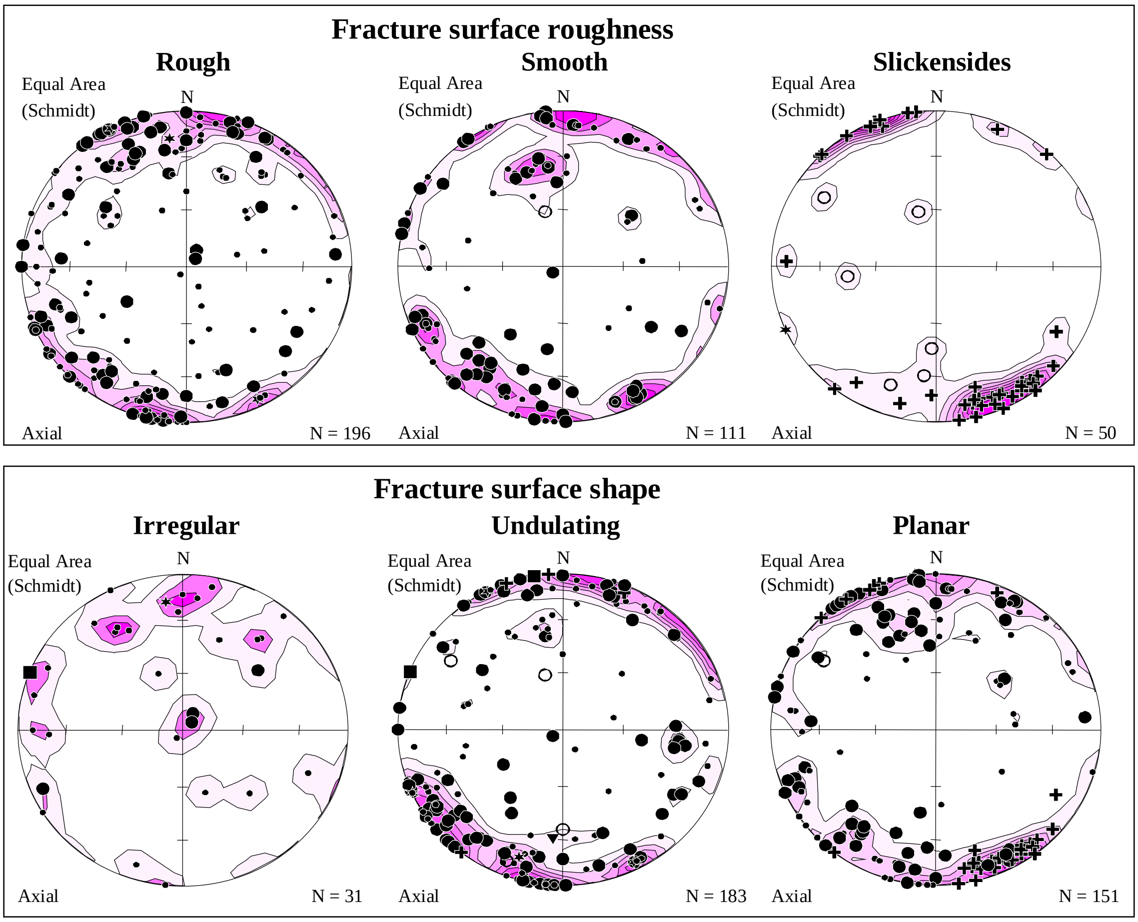

Figure 6.6 Fracture surface roughness and shape of the fracture plane illustrated on stereographic projections.

6.4 Aerial photo interpretations

Fracture traces were visible on aerial photos of the area. Especially along the coast and on some small Islands close to the shore. These fractures and faults were visualy inspected during the fieldwork and has thus been confirmed as being either large fractures or faults. The shape of the islands and the coastline clearly outlines the primary structures. Especially the major thrust fault that truncate the area from NE towards SW. Other outcrops on top of the hills were nicely exposed, and some of the major faults were also verified on the nine measured locations.

Fracture/fault zones are regarded to be more weathered and thus deeper eroded than the sorrounding areas. Characteristic elongated geomorphological depresssions may thus represent such highly fractured zones. They appear as dark lower areas on the aerial photos and they were verified using stereoscopic analysis of overlapping aerial photos and detailed topographical maps.

The results are shown on figure 6.7. The different fractures and faults have directions that may be correlated to the fault directions measured on the 9 locations. Especially the island north of the area provide exceptional possibilities to study three major fault directions that seems to be assocciated with three different tectonic events, related to deformation phase 3-6 and 8 in the next chapter. Other fault zones with an unclear relation have been marked with green on figure 6.7.

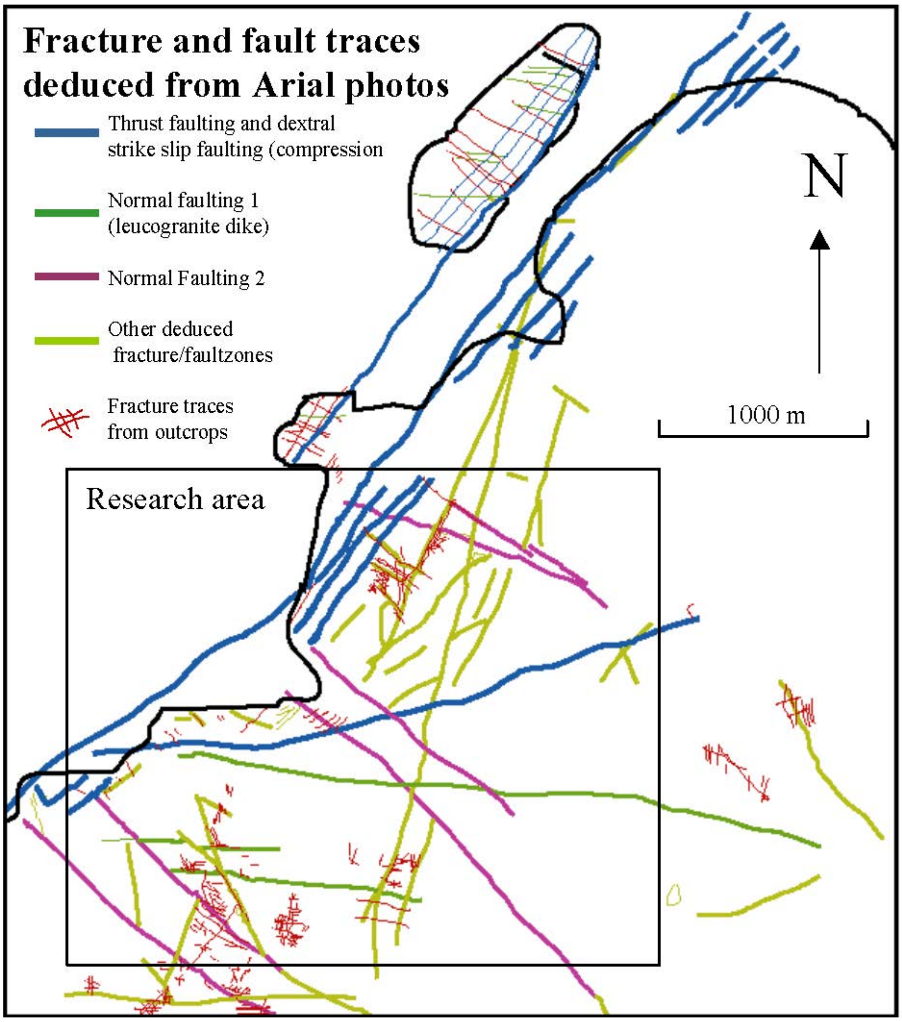

Figure 6.7 Map showing the fracture traces on outcrops deduced from Arial photos.

6.5 Event stratigraphy

Based on the observations from the nine localities the following stratigraphic history may be deduced from the order of events:

1. Granodiorite intrusion at relative large depth. Related to orogenic plate tectonic event.
2. NW-SE extension and intrusion of coarse grained dike (50-25^0/60-70 NW).
3. Lateral compression NW-SE and regional uplift. This event is probably related to the thrust faulting of the Pre-Quaternary meta-sedimentary rocks onto the Hercynic intrusive granodiorite, at location. Strike slip dextral faulting (striking 70-90^0) may be related to this event.
4. Uplift and extension NNE-SSW, intrusion of leucogranite (striking 100-106^0).
5. Reverse faulting at location 5.

6. Normal faulting (striking 90-110^0, dipping 80-60^{0}NE) mayby due to stress release after the intrusion of the leucogranite.
7. Sub-horizontal dome shaped sheet fractures, probably formed as a result of stress release and contraction during further uplift and cooling.
8. Faulting in the valley (geological map figure 1.1) and lines on the islands north of the area striking 130^0 indicate a second faulting event.
9. Weathering and erosion to present day level with deposition of the sediments in the valleys.

These events are correlated to the regional events taking place in the area in table 6.3

Time period	**Regional History**	**Local Event Stratigraphy**	
Pre-Cambrian	Sedimentation	Pre-Cambrian Sedimentation and deformation	
410-390 MA (Late Silurian to Early Devonian)	Iberian peninsula drift towards Laurussia closing the Merrimack Ocean. Dextral transform faulting in northern Iberian peninsula	Folding and faulting of Pre-Cambrian meta-sediments.	
375 MA (Middle Devonian)	Iberian Peninsula Merged with Laurussia. Gondwanaland is drifting towards the Iberian peninsula closing the Tethys Ocean.	Folding and faulting of Pre-Cambrian meta-sediments.	
335-310 MA: Carboniferous Early Visan-Namuirense	Variscian Orogeny. Development of the central Iberian fold-belt with dextral transform shear. + dextral transform deformation.	1'st deformation Phase	<u>Granodioritic intrusion</u> at large depth (large crystals) Extension. Dykes with large crystals intrudes granodiorite (striking 50^0) at location 7.
310-270 MA Late Carboniferous. Westphalian	Closing of the Thethys ocean complete and formation of the supercontinent Pangea is complete.		Stress release during uplift and cooling (non-systematic fractures) <u>Lateral compression NW-SE. dextral strike slip faulting</u> at location 5, 6, 9 and 7. And <u>thrust faulting</u> at location 5.
270-260 MA: Permo-Carboniferous, Estephanienese	Extensional faulting.	2'nd deformation phase	<u>Extension: Intrusion of fine-grained Leucogranite</u> dikes in the granodiorite at relative shallow depth (fine-grained rock) and formation of a Lacolith intrusion over the Granodiorite. <u>Normal faulting</u> (striking 90-100^0) that truncates the strike slip faults and some dikes.
260-250 MA Early Permian	Rifting and formation of the Cantabrian Sea. Extension NE-SW	3'rd deformation phase	Large faults in the valley. (striking 110-130^0) according to the geological map.

Table 6.3 Geological history of the area with interpreted correlation to regional tectonic events in the region.

7. Summary

A contaminated site situated on fractured granitic rocks in Northern Spain was investigated in great details, and a geological model has formed the background for evaluating
The region is highly dominated by meta-sedimentary rocks of Pre-Cambrian age which have been intensively folded and intruded by rocks of primarily granitic origin during the Hercynic fold phase from Early Devonian to Early Permian time.

The Pre-Cambrian meta-sediments are dominating the western part of the area. The meta-sediments consist of conglomerates and quarzites which are locally intruded by amfibolite. The rocks are separated from the Carboniferous intrusions by a large thrust-fault (figure 1.1), that truncate the area from south-west to north-east and dips towards north-west. Three different rocks of granitic composition appear east of the thrust fault, namely two different intrusions of granodiorite, and a fine-grained Leucogranite. The valley floors are covered by different types of primarily sandy deposits of Quaternary age.

The geological history of the Spanish site includes a long history of geological events. At least nine different tectonic events have thus affected the area since the granite was intruded some 400 mill. years ago. These events may be related to regional plate tectonic events that resulted in systematic faults, intrusions and fractures. Local uplift and cooling events created non-systematic fracture systems, and subsequent weathering created zones of deeply weathered granite, primarily in fracture/fault zones. The granite is a non-stratabound overall homogenous rock. It fractures quite heterogeneous and is thus expected to contain very different hydraulic conditions in different regions.

The fracture data collected from Spanish site have been analysed. The degree of fracturing is highly heterogeneous with areas of low fracturing, intersected by zones of highly fractured granite with potentially high hydraulic conductivity. The different types of fractures, dykes and faults has been classified according to the origin of the fractures.

Quantitative values of fracture density in various areas has facilitated an estimation of typical fracture density in fresh granite and in fracture zones. The weathered granite consists of loose unconsolidated “gravel like” rock with a potential high hydraulic conductivity, and the valley floors are covered with sandy deposits.

The area consists thus of four characteristic potential hydraulic homogenous areas: Fresh granite, fracture/fault-zones, weathered granite and sedimentary cover in the valleys.

The heterogeneity of the area complicate the construction of a very accurate hydraulic model, since areas covered with vegetation offer little information about the geological conditions, but there seems to be a connection between the geomorphology and the distribution of fracture zones and weathered granite. Additional detailed analysis of aerial photos may therefore be a valuable tool for the construction of a more detailed model.

References

Bosscher J.P., & Connel D. E., 1988: Measurement and Analysis of Jointing Properties in Fine-grained Soils. in Journal of Geo-technical Engineering, Vol. 114, No. 7, pp 826-843.

Davis G.H., 1984: Structural Geology of rocks and Regions. John Wiley & Sons Inc. pp 342-344.

Kazi A., & Knill J.L. 1973: Fissuring in Glacial Lake Clays and Tills on the Norfolk Coast, United Kingdom. Engineering Geology, Vol. 7 pp. 35-48.

Klint K.E.S., & Fredericia J.: 1998: *Quantitative Fracture Characterisation in Clayey Diamict Sediments. "A Recipe"* Extended abstract in: Mass Transport in Fractured Aquifers and

Klint K.E.S., and Tsakiroglou C.D., 2000: *A New Method of Fracture Aperture Characterisation*. In Protection and Restoration of the Environment V. Proceedings of an International Conference, Thassos, Greece, Ed: V.A. Tsihrintzis, G.P. Korfiatis, K.L. Katsifarakis, A.C. Demetracopoulos. Vol 1. Pp. 127-136.

Nemec, W., 1988: The shape of the Rose. Sedimentary geology, 59 pp. 149-152.

Robin P.Y.F. and Jowett E.C. (1986) Computerised density contouring and statistical evaluation of orientation data, using counting circles and continuos weighting functions. Tectonophysics, Vol. 121, pp. 207-223.

Rosenbom A.E., Hansen M., Klint K.E.S.K., Lorentzen H.J. and Springer N. 2001: Image and SEM-analysis of Fractures in Granite. In: TRACe-Fracture. Toward an Improved Risk Assessment of the Contaminant Spreading in Fractured Underground Reservoirs. GEUS Progress report no 38.

Ziegler P.A. 1989: Evolution of Laurussia: A study in late Palaeozoic Plate Tectonics. Kluwer Academic Publishers, Dordrecht/Boston/London, p 101.

Appendix 1

Geological profiles

Profile 1
Profile 3
Profile 6
Profile 8
Profile 9

Profil 1

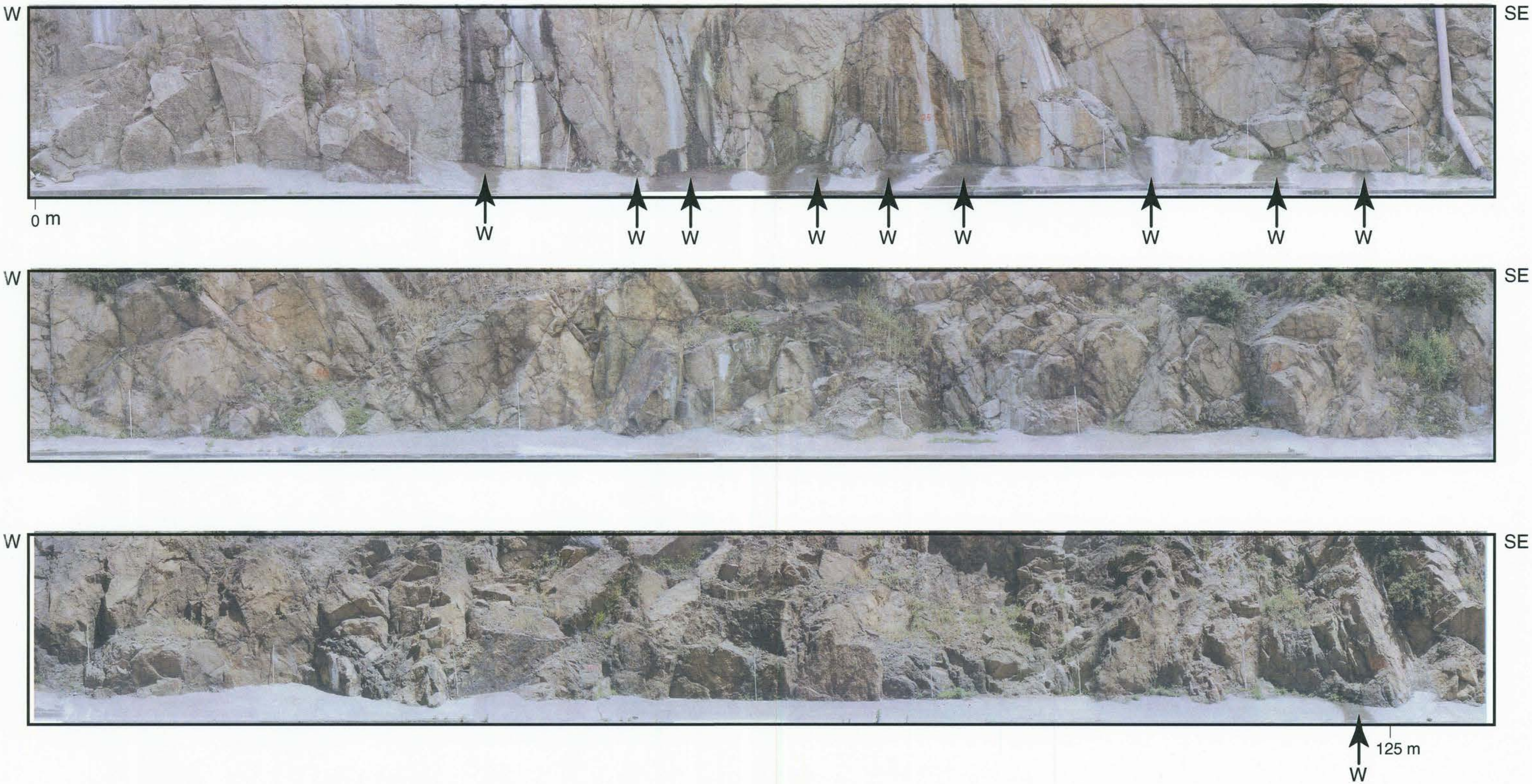

Profil 1

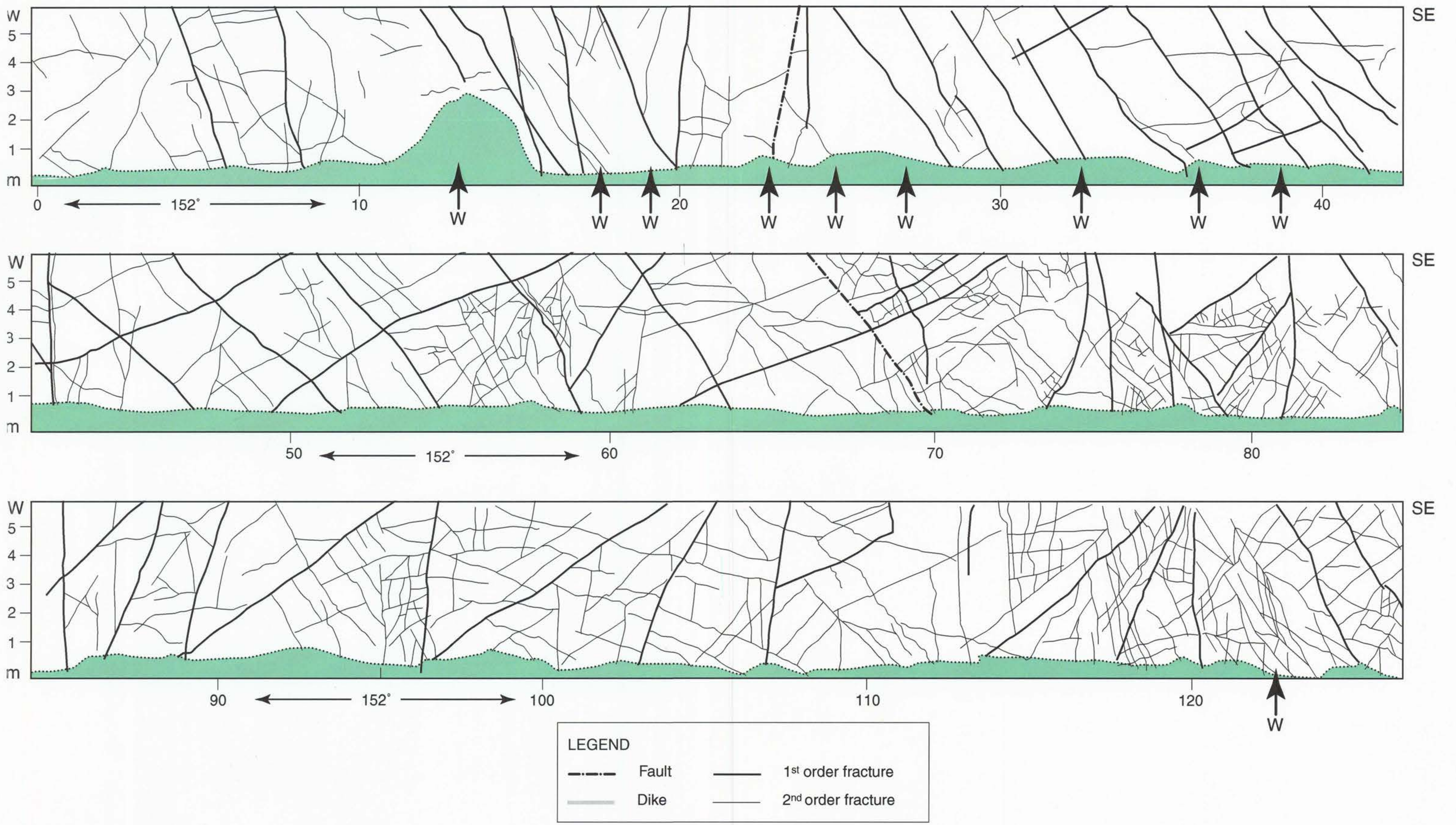

W
SE
m
5
4
3
2
1
0
10
20
30
40
50
60
70
80
90
100
110
120
152°
LEGEND
Fault
Dike
1st order fracture
2nd order fracture

Profil 3

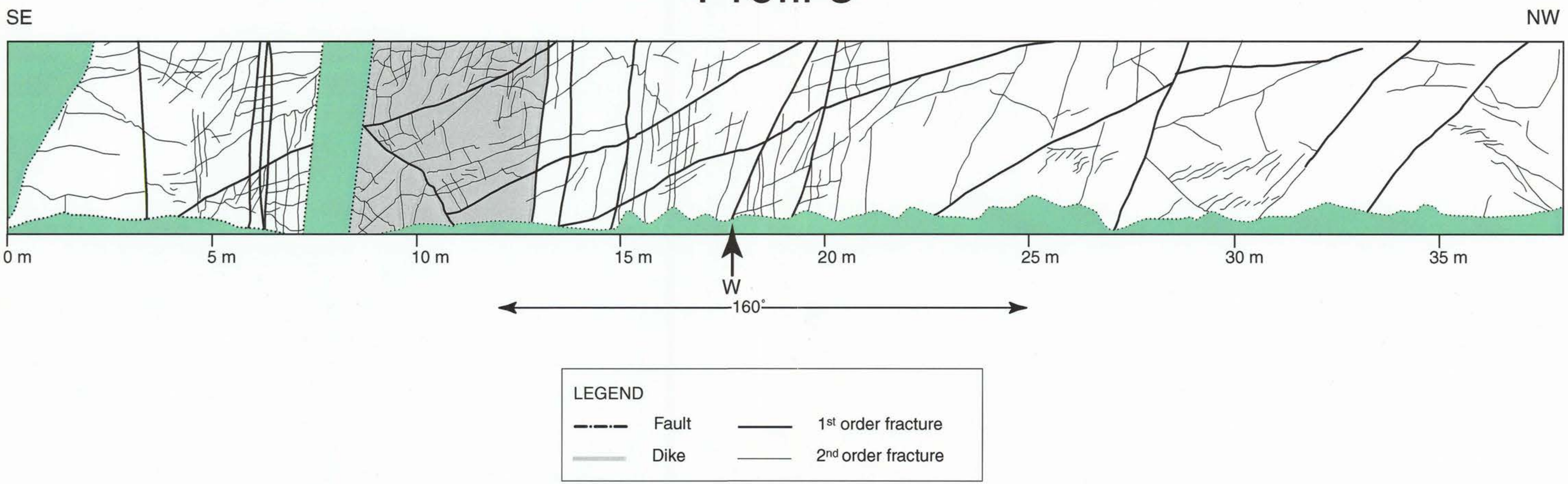

SE
NW
0 m
5 m
10 m
15 m
20 m
25 m
30 m
35 m
W
160°
LEGEND
Fault
1st order fracture
Dike
2nd order fracture

Profil 6


SE
NW
A
B
E
0
10
30
40
40

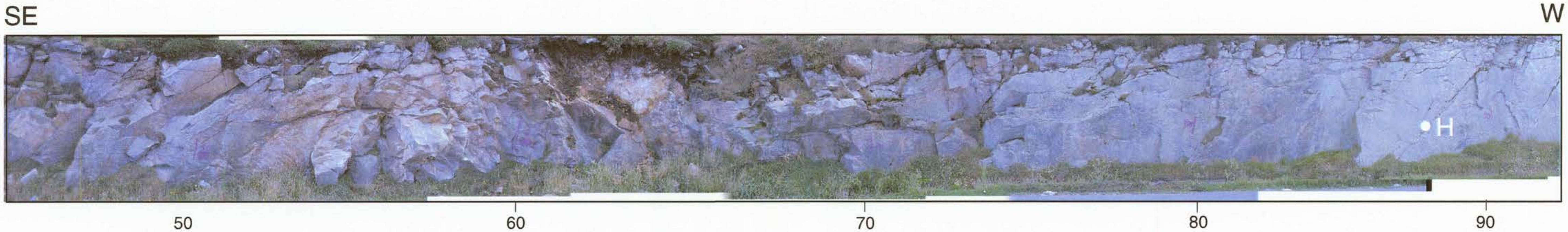
SE
W
H
50
60
70
80
90

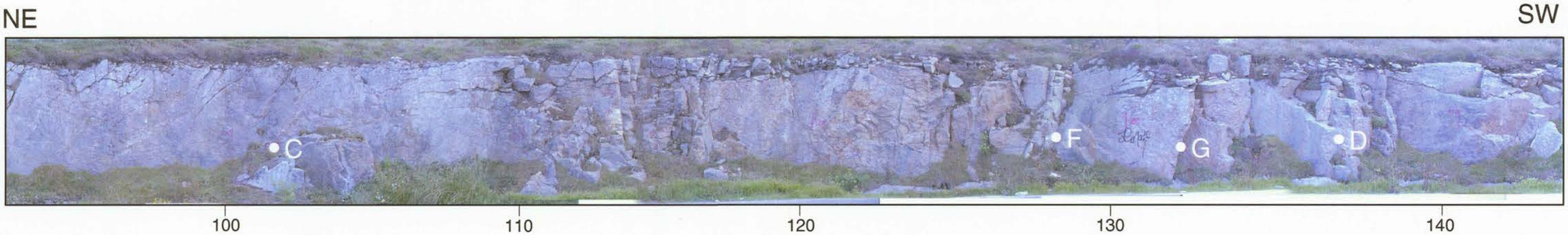
NE
SW
C
F
G
D
100
110
120
130
140


NE
SW
150
160
170
180 m

Profil 6

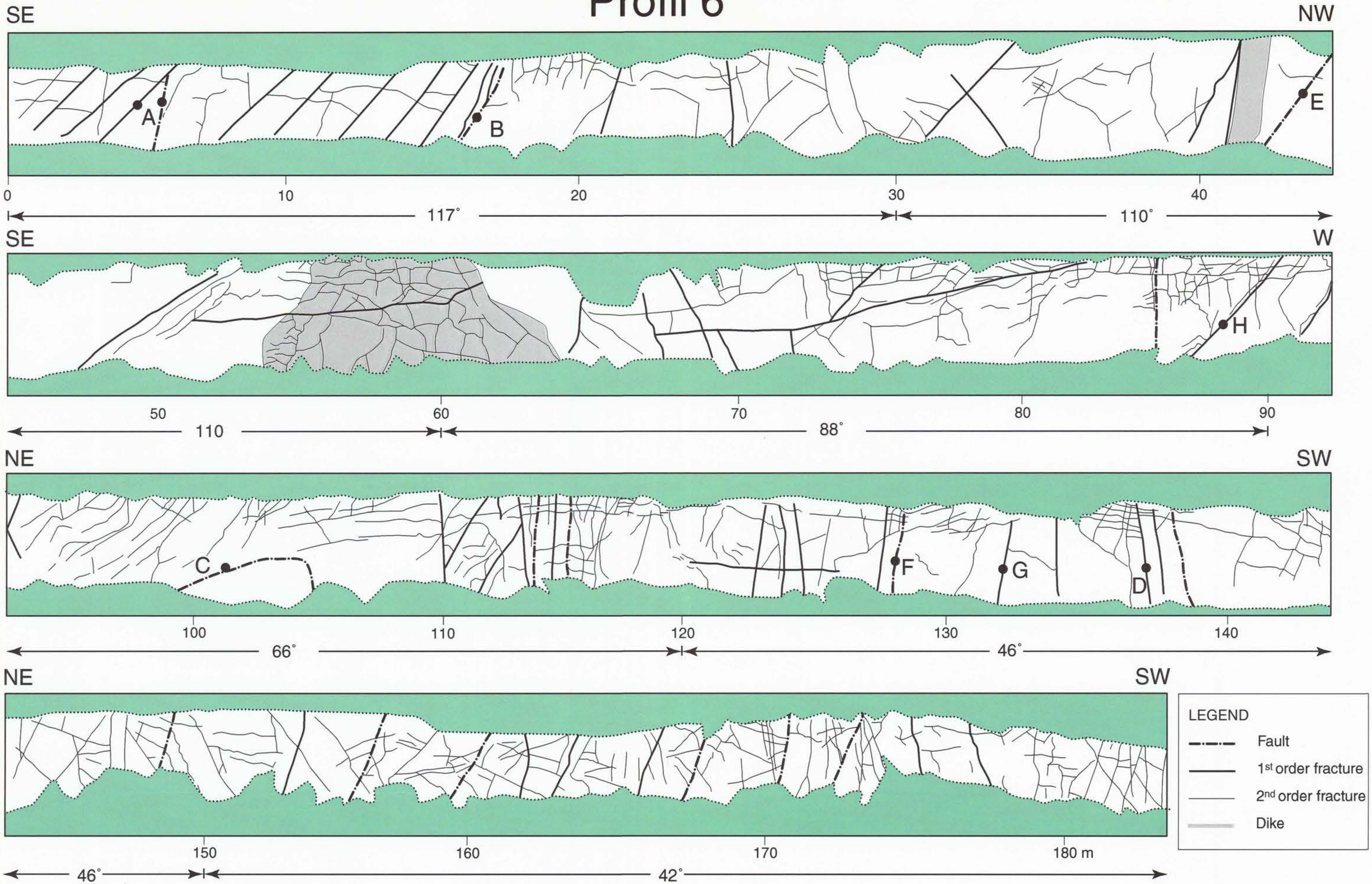
SE
NW
A
B
E
0
10
20
30
40
117˚
110˚
SE
W
H
50
60
70
80
90
110
88˚
NE
SW
C
F
G
D
100
110
120
130
140
66˚
46˚
NE
SW
150
160
170
180 m
46˚
42˚
LEGEND
Fault
1st order fracture
2nd order fracture
Dike

Profi 8

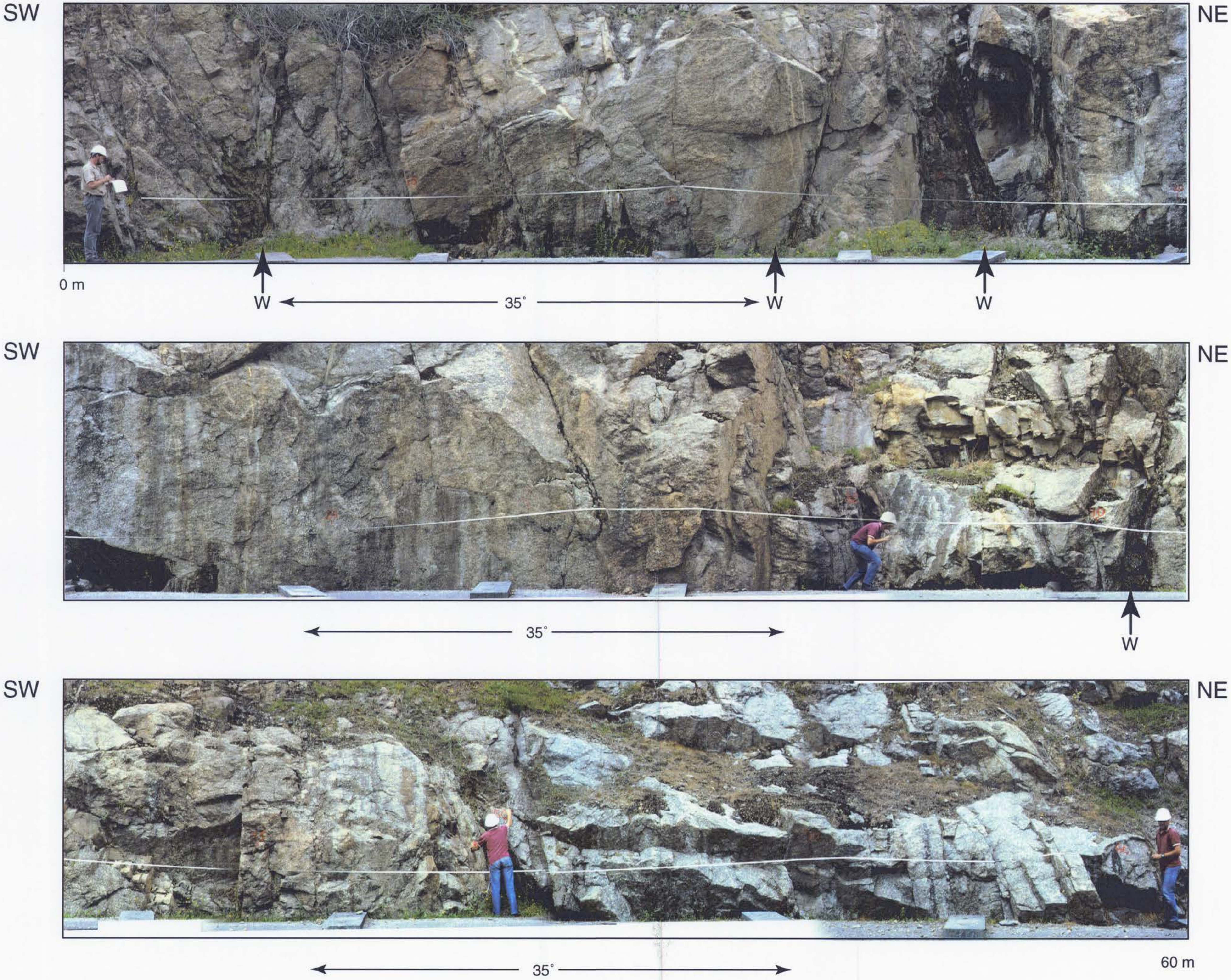

Profi 8

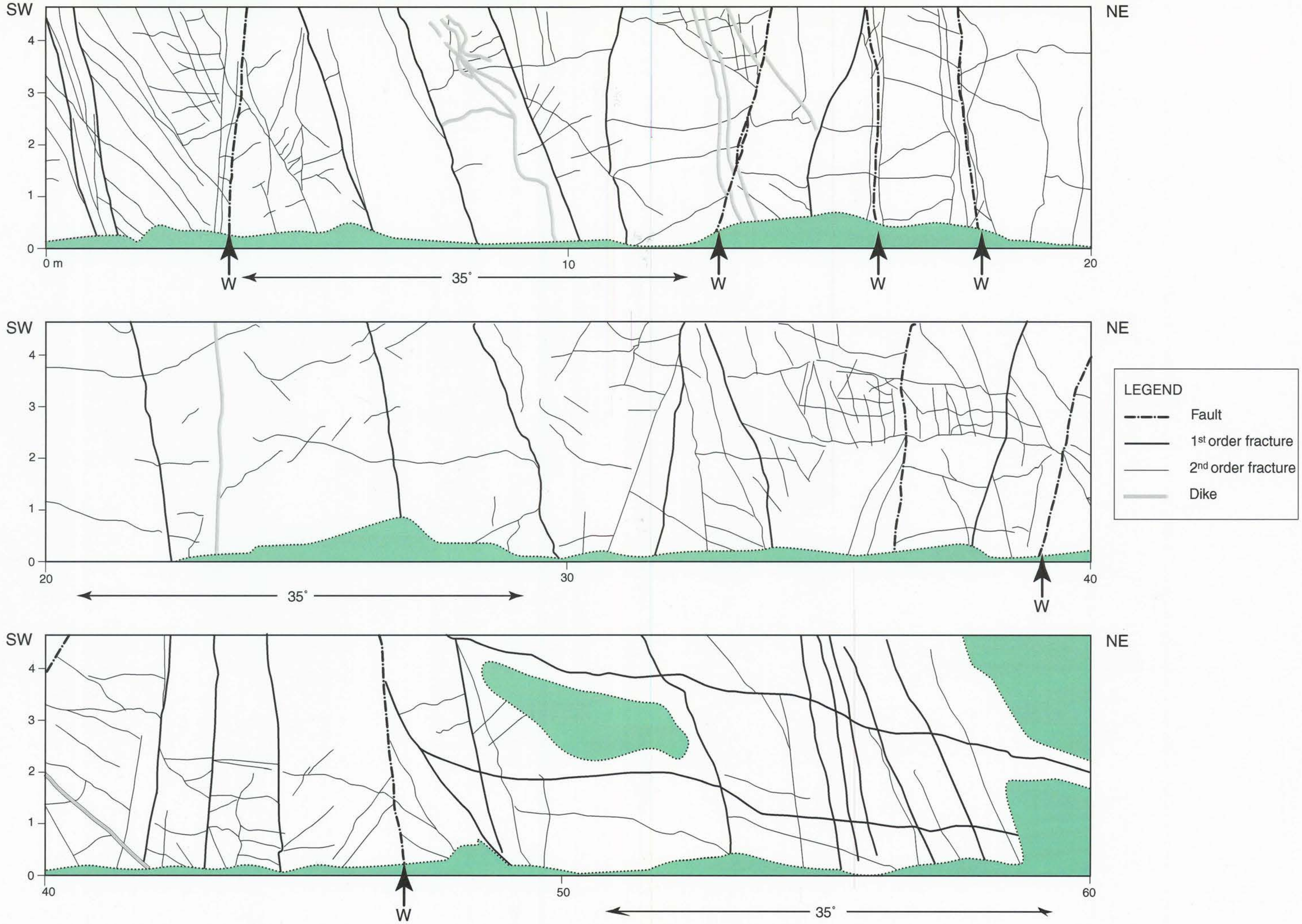

SW
NE
4
3
2
1
0
0 m
10
20
W
35˚
W
W
W
30
40
W
50
60
LEGEND
Fault
1st order fracture
2nd order fracture
Dike

Appendix 2

Profiles 1-9
Fracture-data from the investigated locations on the Spanish site.
All measurements are measured as dip/direction.

Location 1

1. 33 1 278 40 "major fractures on location 1 after 100 m"
2. 33 1 286 40
3. 33 1 36 90
4. 33 1 92 60
5. 33 1 76 90
6. 33 1 266 51
7. 33 1 145 56
8. 33 1 280 46
9. 33 1 168 56
10. 33 1 158 40
11. 33 1 190 80
12. 33 1 82 90
13. 33 1 260 75
14. 33 1 184 64
15. 33 9 160 90 "pl sl sinestral lineation 250 10"
16. 33 1 350 80
17. 33 1 20 85
18. 33 1 226 60
19. 33 1 354 80
20. 33 1 35 90
21. 33 1 3 90
22. 33 1 199 90
23. 33 1 30 90
24. 33 1 230 50
25. 33 1 211 71 "pl ro
26. 33 2 218 85 "on ro"
27. 33 2 153 61 "ir ro"
28. 33 2 147 64 "ir ro"
29. 33 1 143 69 "pl ro"
30. 33 2 178 65 "ir ro"
31. 33 2 142 76 "ir ro"
32. 33 1 306 56 "li sm"
33. 33 1 65 66 "on ro"
34. 33 2 71 90 "on ro"
35. 33 1 67 90 "on ro"
36. 33 2 184 78 "pl sm"
37. 33 2 128 44 "pl ro"
38. 33 1 180 70 "pl ro"
39. 33 1 123 74 "pl ro"
40. 33 2 138 53 "on sm"
41. 33 1 128 52 "on ro water "
42. 33 2 290 70 "ir ro"
43. 33 1 66 82 "ir ro"
44. 33 2 201 52 "ir ro"
45. 33 9 319 83 "pl sl 229/5 sinestral"
46. 33 9 173 90 "pl sl 256/6"
47. 33 2 341 35 "ir ro"
48. 33 2 185 80 "on ro"
49. 33 2 35 5 "ir ro"
50. 33 2 186 70 "on ro"
51. 33 2 219 65 "ir ro"
52. 33 2 218 63 "ir ro"
53. 33 1 70 80 "pl sm"
54. 33 2 158 32 "ir ro"
55. 33 1 170 51 "on ro"
56. 33 2 175 63 "on ro"
57. 33 2 154 56 "on sm"
58. 33 1 73 72 "pl ro"
59. 33 1 66 90 "pl ro"
60. 33 2 340 22 "li ro water"
61. 33 1 153 53 "pl sm"
62. 33 2 74 53 "on ro"
63. 33 2 330 12 "on ro"
64. 33 2 198 90 "on ro"
65. 33 2 325 40 "on sm"
66. 33 2 139 54 "pl ro"
67. 33 1 143 90 "pl sm"
68. 33 2 90 80 "ir ro"
69. 33 2 230 40 "pl ro"
70. 33 2 70 70 "on ro"
71. 33 2 38 75 "on ro"
72. 33 2 354 60 "on ro"
73. 33 2 212 83 "on ro"
74. 33 2 166 57 "on sm"
75. 33 2 22 70 "on ro"
76. 33 1 196 86 "on ro"
77. 33 2 201 80 "on ro"
78. 33 2 80 50 "on ro"
79. 33 31 163 30 "on sm dip/slip fault"
80. 33 1 172 54 "pl sm"
81. 33 1 160 54 "pl sm"
82. 33 1 42 90 "pl sm"
83. 33 2 83 80 "on ro"
84. 33 2 205 80 "on sm"
85. 33 2 218 86 "on sm"
86. 33 2 172 50 "on ro"
87. 33 1 302 68 "on ro"

88. 33 2 170 61 "on sm"
89. 33 9 300 73 "pl sl 220/46"
90. 33 1 70 83 "on ro"
91. 33 2 296 56 "on ro precipitation"
92. 33 2 180 90 "pl ro precipitation"
93. 33 1 150 90 "on ro"
94. 33 2 256 26 "on ro"
95. 33 2 104 52 "on ro"
96. 33 2 186 74 "ir ro"
97. 33 2 38 90 "on ro"
98. 33 2 220 85 "ir ro"
99. 33 3 30 90 "dyke"
100.33 31 119 90 "normal fault "
101.33 1 98 90 "on ro"
102.33 2 38 80 "on ro"
103.33 13 49 80 "15 fractures 70 cm wide fracturezone"
104.33 2 199 85 "on ro"
105.33 2 344 60 "on ro"
106.33 3 34 90 "dyke"
107.33 2 44 90 "on sm"
108.33 2 20 90 "on ro"
109.33 1 170 80 "on ro"
110.33 2 180 40 "on ro"
111.33 -2 62 90 "strike of profile"
112.33 3 355 80 "dyke young"
113.33 3 150 40 "dyke old (truncated by "112)"

Location 2

Beach locality

1. 33 9 3.0 135 90 "dextral strike slipfault 235-8 (slickenside) location 2"
2. 33 1 2.0 156 75 "pl ro"
3. 33 1 2.0 160 85 "pl ro"
4. 33 1 2.0 148 90 "pl ro"
5. 33 1 2.0 170 65 "pl ro"
6. 33 1 2.0 184 80 "pl sm"
7. 33 1 2.0 232 44 "pl sm"
8. 33 1 2.0 4 65 "pl sm"
9. 33 1 2.0 0 72 "locality 2 by the beach. on ro. scan-line 165 degree"
10. 33 1 2.0 16 76 "0n ro"
11. 33 2 1.0 37 50 "0n ro"
12. 33 2 1.0 38 65 "0n ro"
13. 33 2 1.0 127 90 "0n ro"
14. 33 1 2.0 0 85 "pl sm very large 2 cm quartz filling"
15. 33 2 1.0 125 90 "pl sm"
16. 33 2 1.0 125 90 "pl sm"
17. 33 1 2.0 174 90 "pl sm very large 1-2 cm quartz filling"
18. 33 9 3.0 175 90 "dextral transform fault 40 cm transition"
19. 33 2 1.0 134 80 "0n ro"
20. 33 2 1.0 50 90 "0n ro"
21. 33 1 2.0 19 90 "0n ro"
22. 33 2 1.0 131 75 "on ro"
23. 33 2 1.0 164 90 "pl ro"
24. 33 1 2.0 155 65 "pl ro"
25. 33 1 2.0 141 90 "pl ro"
26. 33 2 1.0 115 80 "0n ro"
27. 33 2 1.0 115 70 "0n ro"
28. 33 2 1.0 58 50 "0n ro"
29. 33 2 1.0 59 90 "new orientation of scan line 2 degree after 14 m"
30. 33 2 1.0 50 90 "fracture zone 12 fractures "
31. 33 1 2.0 44 70 "0n ro"
32. 33 2 1.0 123 50 "0n ro"
33. 33 2 1.0 40 90 "0n ro"
34. 33 2 1.0 6 90 "pl ro"
35. 33 2 1.0 128 90 "on ro"
36. 33 2 1.0 98 75 "pl sm"
37. 33 2 1.0 46 90 "0n ro"
38. 33 2 1.0 1 90 "pl ro"
39. 33 1 2.0 176 45 "pl sm"
40. 33 2 1.0 304 40 "pl sm"
41. 33 1 2.0 41 80 "quartz filling"
42. 33 1 2.0 45 90 "on ro"
43. 33 2 1.0 158 40 "pl sm"
44. 33 2 1.0 89 70 "pl sm"
45. 33 1 2.0 332 76 "on ro"
46. 33 1 2.0 312 70 "on ro"
47. 33 2 1.0 146 70 "0n ro"
48. 33 2 1.0 41 90 "on ro"
49. 33 2 1.0 240 65 "0n ro"
50. 33 2 1.0 234 40 "pl sm"
51. 33 2 1.0 167 90 "on ro"

Location 3

1. 33 1 292 78 "scanline 150 degree location 3 "
2. 33 1 46 60 "pl sm"
3. 33 2 276 76 "on ro"
4. 33 2 64 74 "on sm"
5. 33 2 76 50 "pl sm"
6. 33 1 330 84 "on sm"
7. 33 1 333 85 "on sm"
8. 33 2 120 44 "on ro"
9. 33 2 266 40 "pl sm"
10. 33 2 192 80 "pl sm"
11. 33 2 202 76 "on sm"

12. 33 2 153 90 "on sm"
13. 33 2 145 90 "on sm"
14. 33 1 333 85 "pl ro fraturezone 5 fractures"
15. 33 1 332 85 "pl sm"
16. 33 2 258 40 "pl ro"
17. 33 1 152 89 "pl ro"
18. 33 2 330 85 "on ro"
19. 33 1 158 90 "on ro"
20. 33 2 35 70
21. 33 3 158 88 "dyke"
22. 33 3 140 85 "other site of dyke 4.4 meter thick"
23. 33 1 143 90 "pl sm"
24. 33 1 145 90
25. 33 2 14 85 "on ro"
26. 33 2 16 90 "on ro"
27. 33 2 38 90 "on ro"
28. 33 1 149 90 "pl ro"
29. 33 1 152 90 "on ro"
30. 33 1 158 85 "on ro"
31. 33 1 153 90 "on ro (spacing 15-20 cm in a 2 meter wide zone)"
32. 33 1 200 80 "on ro"
33. 33 1 12 90 "on ro"
34. 33 1 198 80 "on ro"
35. 33 1 10 90 "pl sm"
36. 33 1 14 90 "on ro"
37. 33 1 66 80 "pl sm"
38. 33 1 165 90 "on ro"
39. 33 2 16 60 "on ro"
40. 33 2 50 80 "on ro"
41. 33 1 8 90 "on ro"
42. 33 1 36 75 "on ro"
43. 33 1 69 90 "orientation of fractures in the dyke location 3"
44. 33 1 60 80 "orientation of fractures in the dyke location 3"
45. 33 1 46 70 "orientation of fractures in the dyke location 3"
46. 33 1 58 85 "orientation of fractures in the dyke location 3"
47. 33 1 56 82 "orientation of fractures in the dyke location 3"
48. 33 1 50 90 "orientation of fractures in the dyke location 3"
49. 33 1 57 80 "orientation of fractures in the dyke location 3"
50. 33 1 49 83 "orientation of fractures in the dyke location 3"
51. 33 1 44 90 "orientation of fractures in the dyke location 3"
52. 33 1 50 75 "orientation of fractures in the dyke location 3"
53. 33 1 50 70 "orientation of fractures in the dyke location 3"
54. 33 1 39 80 "orientation of fractures in the dyke location 3"
55. 33 1 275 60 "orientation of fractures in the dyke location 3"
56. 33 1 268 58 "orientation of fractures in the dyke location 3"
57. 33 1 278 58 "orientation of fractures in the dyke location 3"
58. 33 1 276 60 "orientation of fractures in the dyke location 3"
59. 33 1 278 64 "orientation of fractures in the dyke location 3"
60. 33 1 280 58 "orientation of fractures in the dyke location 3"
61. 33 1 5 90 "orientation of fractures in the dyke location 3"
62. 33 1 3 90 "orientation of fractures in the dyke location 3"

Location 4

1. 33 1 94 90
2. 33 2 22 80
3. 33 2 30 80
4. 33 2 142 70
5. 33 2 145 70
6. 33 1 50 90
7. 33 1 18 72
8. 33 2 288 75
9. 33 1 96 88
10. 33 1 100 90
11. 33 1 92 90
12. 33 2 36 80
13. 33 2 12 90
14. 33 2 194 75
15. 33 2 10 90
16. 33 2 6 90
17. 33 2 30 70
18. 33 1 282 84
19. 33 2 145 90
20. 33 1 244 74
21. 33 2 120 88
22. 33 1 100 70
23. 33 1 12 90
24. 33 2 170 89
25. 33 1 104 90
26. 33 2 68 60
27. 33 1 262 90
28. 33 2 352 85
29. 33 2 18 68

30. 33 2 5 70
31. 33 2 256 20
32. 33 2 7 70
33. 33 2 169 90
34. 33 2 10 88
35. 33 2 171 82
36. 33 2 62 89
37. 33 2 76 86
38. 33 2 3 90
39. 33 2 78 80
40. 33 2 56 68
41. 33 2 35 75
42. 33 1 297 80
43. 33 1 235 78
44. 33 2 260 70
45. 33 2 235 72
46. 33 2 65 85

Location 5

Coastal cliffs north of beach

1. 33 -2 5 60 "revers fault at location 5, the coastal rocks."
2. 33 -2 9 43 "reverse fault"
3. 33 -2 350 50 "reverse fault"
4. 33 -2 334 52 "reverse oblique fault"
5. 33 -2 336 46 "reverse oblique fault"
6. 33 -2 14 55 "transform dextral fault"
7. 33 -2 316 71 "transform dextral fault"
8. 69 1 46 45 "slickenside"
9. 69 1 55 28 "slickenside"
10. 69 1 45 30 "slickenside"
11. 69 1 45 21 "slickenside"
12. 69 1 50 12 "slickenside"
13. 69 1 230 8 "slickenside"
14. 33 -2 140 90 "best fit greatcircle for the slickensides"

Location 6

Roadcut south of beach

1. 33 31 123 70 "normal fault pl sl, lineaton 114/70"
2. 33 2 6 90 "ir ro"
3. 33 1 172 87 "pl sm"
4. 33 2 23 82 "on ro"
5. 33 2 191 83 "ir ro en echelon"
6. 33 1 173 72 "ir ro 7 fractures "
7. 33 2 315 48 "ir ro"
8. 33 31 83 45 "on sl oblique fault lineation 10/20"
9. 33 9 160 85 "on sl lineation 248/8"
10. 33 9 170 90 "on sl lineation 264/8"
11. 33 2 110 90 "on ro"
12. 33 3 6 90 "5 cm thick dyke"
13. 33 1 166 78 "on ro 2 cm quartz filling"
14. 33 2 225 42 "on ro"
15. 33 31 22 50 "normal fault lineation 2/45"
16. 33 1 211 85 "pl ro"
17. 33 9 92 80 "on sl, sinestral lineation 181/5"
18. 33 2 185 80 "pl sm"
19. 33 3 112 90 "dyke 80 cm thick, irregular contact"
20. 33 2 88 70 "ir ro"
21. 33 31 20 70 "on sl, lineation 344/46"
22. 33 2 180 76 "ir ro"
23. 33 1 90 90
24. 33 2 186 80 "pl sm"
25. 33 2 180 70 "pl ro"
26. 33 2 71 70 "pl ro"
27. 33 1 10 72 "on ro"
28. 33 3 170 90 "one side of dyke 2 meter wide"
29. 33 3 146 75 "other side of the same dyke"
30. 33 3 188 70 "dyke 50 cm wide"
31. 33 3 52 90 "dyke"
32. 33 1 206 80 "pl sm"
33. 33 1 180 70 "pl ro"
34. 33 2 64 80 "pl ro"
35. 33 1 265 80 "pl ro"
36. 33 9 334 75 "dextral transform fault"
37. 33 9 330 82 "dextral transform fault"
38. 33 1 50 80 "on ro"
39. 33 9 332 77 "dextral transform fault"
40. 33 31 0 54 "normal fault along dyke cutting transform fault"
41. 33 2 0 90 "on ro"
42. 33 3 350 48 "dyke 50 cm thick"
43. 33 9 338 90 "dextral transform fault"
44. 33 2 40 90 "on sm"
45. 33 9 336 90 "dextral transform fault. slickenside 66/12"
46. 33 9 333 80 "dextral transform fault"
47. 33 1 106 90 "pl sm"
48. 33 1 120 90 "pl sm"
49. 33 2 258 80 "on ro"
50. 33 9 357 90 "dextral transform fault"
51. 33 9 343 85 "dextral transform fault"
52. 33 2 16 72 "on ro"
53. 33 1 107 88
54. 33 2 110 90 "pl sm"
55. 33 9 156 90 "dextral transform fault"
56. 33 1 58 35 "on ro"

57. 33 9 156 90 "dextral transform fault"
58. 33 2 286 89 "pl sm"
59. 33 1 330 78 "pl sm"
60. 33 1 102 90 "pl sm"
61. 33 2 106 50 "on sm"
62. 33 2 24 73 "on sm"
63. 33 2 285 80 "on sm"
64. 33 9 160 90 "dextral transform fault"
65. 33 9 170 90 "dextral transform fault"
66. 33 9 163 90 "dextral transform fault"
67. 33 2 250 85 "on ro"

Location 7

1. 33 1 340 60 on ro"
2. 33 9 340 80 "dextral transform fault off-setting dyke 40 cm"
3. 33 9 338 90 "dextral transform fault"
4. 33 9 349 80 "dextral transform fault"
5. 33 1 346 79 "on ro"
6. 33 9 344 69 "dextral transform fault"
7. 33 3 294 70 "dyke 5 cm wide"
8. 33 2 57 65 "on ro"
9. 33 2 36 68 "pl ro"
10. 33 2 66 90 "on ro"
11. 33 1 34 70 "pl ro"
12. 33 2 217 65 "pl ro"
13. 33 2 198 55 "pl ro"
14. 33 2 203 52 "pl ro"
15. 33 2 15 90 "on ro"
16. 33 2 19 80 "on ro"
17. 33 2 10 90 "on ro"
18. 33 2 13 70 "on ro"
19. 33 31 0 50 "normal fault"
20. 33 31 10 90 "normal fault"
21. 33 31 18 60 "normal fault"
22. 33 31 10 68 "normal fault"
23. 33 2 104 82 "ir ro"
24. 33 1 2 86 "lp ro"
25. 33 31 0 65 "normal fault"
26. 33 2 24 80 "pl sm"
27. 33 1 230 50 "ir ro"
28. 33 31 6 60 "normal fault slickenside 20/60"
29. 33 1 210 10 "ir ro dome shaped (maby stress release)"
30. 33 1 228 6 "ir ro etc."
31. 33 1 211 1
32. 33 1 56 6 "on sm"
33. 33 2 176 80 "on sm"
34. 33 3 37 75 "dyke 8 cm thick"
35. 33 1 14 80 "poss. conjugating with 36-38"
36. 33 2 214 80 "pl sm"
37. 33 2 209 82 "pl sm"
38. 33 2 207 81
39. 33 2 214 81 "en echelon" fractures"
40. 33 2 217 86 "etc."
41. 33 2 213 83 "etc."
42. 33 31 18 75 "orientation of fracturezone with en echelon fractures"
43. 33 1 41 90 "on sm"
44. 33 1 228 80 "mega-fracture extensionel with syntaxial growth of quartz "
45. 33 1 34 68 "pl sm"
46. 33 1 40 68 "pl sm"
47. 33 1 35 65 "pl sm same system as 45-46"
48. 33 1 8 80 "pl sm"
49. 33 1 356 70 "pl sm"
50. 33 1 12 70 "pl sm same system as 48-49"
51. 33 2 182 50 "pl sm"
52. 33 3 292 70 "dyke 10 cm"
53. 33 1 180 89 "on ro"
54. 33 9 18 90 "transform fault"

Location 8

1. 33 1 359 90 "on sm location 8"
2. 33 3 153 90 "dyke"
3. 33 1 36 45 "on sm"
4. 33 1 30 52 "on o"
5. 33 9 36 90 "fault. Water sepage"
6. 33 2 18 80 "ir ro"
7. 33 2 340 82 "on sm"
8. 33 1 33 78 " pl ro"
9. 33 1 126 79 "on sm"
10. 33 2 17 80
11. 33 1 18 75
12. 33 1 24 76 "on sm"
13. 33 2 36 34
14. 33 3 352 75 "dyke"
15. 33 2 210 82
16. 33 1 33 74 "on sm"
17. 33 2 58 90 "on sm"
18. 33 2 270 60 "##"
19. 33 1 273 80 "##"
20. 33 31 203 80 "normal fault"
21. 33 1 70 85 "pl sm"
22. 33 2 300 28 "##"
23. 33 2 152 60 "on sm"

24. 33 2 240 55 "##"
25. 33 3 22 80 "1 m thick faultzone with 12 fractures/faults, Water sepage"
26. 33 3 18 85 "fault"
27. 33 2 172 55 "on sm"
28. 33 2 3 90 "on sm"
29. 33 2 81 35 "##"
30. 33 2 12 90 "##"
31. 33 2 154 90 "on sm"
32. 33 2 24 90 "##"
33. 33 1 149 80 "##"
34. 33 2 116 80 "ir ro"
35. 33 1 66 90 "pl sm"
36. 33 2 59 80 "pl sm"
37. 33 2 58 90 "ir ro"
38. 33 2 64 80 "on sm"
39. 33 2 69 83 "##"
40. 33 2 184 68 "##"
41. 33 2 69 80 "##"
42. 33 9 38 90 "strike slip fault 57 cm displacement. on sl."
43. 33 3 0 70 "dyke"
44. 33 1 37 76 "on sm "
45. 33 2 58 80 "on sm"
46. 33 1 46 90 "water sepage"
47. 33 1 20 60 "pl sm"
48. 33 2 52 90 "pl sm"
49. 33 2 2 80 "##"
50. 33 2 246 80 "pl sm"
51. 33 2 242 80 "pl sm"
52. 33 1 230 90 "##"
53. 33 1 294 80 "##"
54. 33 1 202 90 "on ro"
55. 33 2 66 80 "on sm"
56. 33 2 6 90 "on sm"
57. 33 2 38 87 "##"
58. 33 2 125 42 "##"
59. 33 2 70 90 "##"
60. 33 2 275 86 "##"
61. 33 2 185 86 "on ro"
62. 33 2 149 66 "ir ro"
63. 33 2 40 76 "pl ro"
64. 33 1 50 68 "##"
65. 33 1 140 60 "##"
66. 33 1 17 88 "##"
67. 33 9 2 72 "strike slip fault"
68. 33 1 14 90 "on ro"
69. 33 1 4 86 "water sepage"
70. 33 1 300 72 "on sm"
71. 33 1 10 90 "pl sm"
72. 33 1 305 60 "##"
73. 33 2 22 80 "pl sm"
74. 33 2 16 78 "pl sm"
75. 33 1 40 80 "pl sm"
76. 33 2 356 70 "##"
77. 33 1 16 78 "##"
78. 33 2 8 86 "0n ro"
79. 33 2 15 85 "on ro"
80. 33 2 16 80 "##"
81. 33 2 20 85 "##"
82. 33 2 38 70 "##"
83. 33 2 300 64 "##"
84. 33 1 352 80 "##"
85. 33 2 44 80 "##"
86. 33 1 316 70 "##"
87. 33 1 14 80 "pl sl"
88. 33 1 54 70 "##"
89. 33 2 320 72 "##"
90. 33 2 49 70 "##"
91. 33 1 3 90 "##"
92. 33 1 130 60 "##"
93. 33 1 136 62 "##"
94. 33 2 52 62 "##"
95. 33 2 36 70 "##"
96. 33 1 68 68 "##"
97. 33 1 140 58 "##"
98. 33 1 132 52 "##"
99. 33 1 136 58 "##"

Location 9

Roadcut south of beach and west of the facility.

1. 33 9 160 90 "pl sl location 6.3 strike of profile 103 degree"
2. 33 1 10 45 "pl sm"
3. 33 31 3 44 "li sl lineation 7/44"
4. 33 9 327 85 "pl sl"
5. 33 2 182 60 "pl sm"
6. 33 9 160 90 "pl sl"
7. 33 9 33 78 "pl sl"
8. 33 9 338 80 "pl sl"
9. 33 2 223 88 "pl sl"
10. 33 9 334 80 "pl sl"
11. 33 9 343 78 "pl sl"
12. 33 9 322 82 "pl sl"
13. 33 9 343 70 "pl sl"
14. 33 9 346 90 "pl sl"
15. 33 9 352 90 "pl sl"
16. 33 9 147 90 "pl sl"
17. 33 9 158 90 "pl sl"
18. 33 1 94 65 "pl ro"
19. 33 2 56 90 "pl ro"
20. 33 2 230 80 "on ro"
21. 33 9 156 88 "pl sl"
22. 33 3 18 64 "pegmatit dyke diskordant to fault"
23. 33 3 162 90 "pegmatit dyke parallel to fault"

24. 33 9 346 80 "pl sl"
25. 33 2 351 80 "on ro"
26. 33 2 332 85 "on ro"
27. 33 2 65 90 "12 en echelon fractures <50 cm long"
28. 33 9 325 80 "pl sl"
29. 33 1 56 90 "on ro"
30. 33 2 154 90 "ir ro"
31. 33 2 55 90 "on ro"
32. 33 9 331 85 "pl sl"
33. 33 1 143 90 "on ro"
34. 33 9 335 80 "pl sl"
35. 33 9 326 82 "pl sl"
36. 33 9 343 83 "pl sl"
37. 33 9 345 78 "pl sl"
38. 33 9 338 85 "pl sl"
39. 33 2 53 90 "9 fractures en echelon spacing 4-5 cm"
40. 33 9 66 90 "on sl shearzone 5 fractures with quartz fill. Granite deformed."
41. 33 2 319 80 "on ro"
42. 33 2 6 90 "on ro"
43. 33 2 3 90 "pl ro"
44. 33 2 55 90 "on ro"
45. 33 2 98 78 "pl ro"
46. 33 2 356 40 "pl ro"
47. 33 9 136 90 "pl sl"
48. 33 9 349 80 "pl sl"
49. 33 9 322 85 "pl sl"
50. 33 9 323 90 "pl sl"
51. 33 1 159 68 "pl ro"
52. 33 1 157 68 "pl ro"
53. 33 1 340 82 "pl sm"
54. 33 1 332 80 "pl sm"
55. 33 2 163 54 "pl sm"
56. 33 1 168 60 "pl sm"
57. 33 2 6 90 "pl sm"
58. 33 2 16 90 "pl sm"
59. 33 2 18 90 "pl sm"
60. 33 2 46 90 "pl ro"
61. 33 1 174 85 "pl sm"
62. 33 1 46 70 "on sm"
63. 33 1 210 85 "pl ro"
64. 33 9 312 85 "pl sl"

Total number of slickensides

69 31 20 60 "slickenside normal fault"
69 5 46 45 "slickenside revers fault"
69 5 55 28 "slickenside revers fault"
69 5 45 30 "slickenside revers fault"
69 5 45 21 "slickenside revers fault"
69 5 50 12 "slickenside revers fault"
69 5 230 8 "slickenside"
69 9 66 12 "slickenside transvers fault"
69 31 7 44 "slickenside normal fault"
69 31 114 70 "slickenside normal fault"
69 31 10 20 "slickenside normal fault"
69 9 248 8 "slickenside transvers fault"
69 9 264 8 "slickenside transvers fault"
69 31 2 45 "slickenside normal fault"
69 9 181 5 "slickenside transvers fault"
69 31 344 46 "slickenside normal fault"
69 9 229 5 "slickenside transvers fault"
69 9 256 6 "slickenside transvers fault"
69 31 220 46 "slickenside normal fault"
69 31 196 10 "slickenside normal fault"
69 9 235 8 "slickenside transvers fault"
69 9 66 12 "slickenside transvers fault"
69 31 80 48 "slickenside normal fault"
69 31 20 60 "slickenside normal fault"
69 9 250 10 "slickenside transvers fault"

Appendix 3

Fracture spacing/intensity data

Location 1												
Strike W	Strike Fr.	Angle A-B	Length W	N 1'st	N 2'nd	N tot	Sp. N 1'st	Sp. N 2'nd	Sp. N tot	Fr. int.1	Fr. Int.2	Fr. Int tot
152	5	27	75	2	1	3	22,70	45,40	12,77	0,04	0,02	0,08
152	15	37	75	0	1	1	0,00	60,18	60,18	0,00	0,02	0,02
152	25	47	75	1	2	3	73,14	36,57	20,57	0,01	0,03	0,05
152	35	57	75	2	2	4	41,93	41,93	16,77	0,02	0,02	0,06
152	45	67	75	2	2	4	46,03	46,03	18,41	0,02	0,02	0,05
152	55	77	75	2	3	5	48,72	27,40	15,22	0,02	0,04	0,07
152	65	87	75	2	5	7	49,93	15,60	10,92	0,02	0,06	0,09
152	75	83	75	2	3	5	49,63	27,92	15,51	0,02	0,04	0,06
152	85	73	75	4	5	9	19,13	14,94	8,07	0,05	0,07	0,12
152	95	63	75	1	6	7	89,10	11,46	9,75	0,01	0,09	0,10
152	105	53	75	1	2	3	79,86	39,93	22,46	0,01	0,03	0,04
152	115	43	75	0	5	5	0,00	10,66	10,66	0,00	0,09	0,09
152	125	33	75	3	9	12	15,32	4,60	3,43	0,07	0,22	0,29
152	135	23	75	1	3	4	39,07	10,99	7,81	0,03	0,09	0,13
152	145	13	75	0	1	1	0,00	22,50	22,50	0,00	0,04	0,04
152	155	3	75	0	0	0	0,00	0,00	0,00	0,00	0,00	0,00
152	165	7	75	0	0	0	0,00	0,00	0,00	0,00	0,00	0,00
152	175	17	75	7	6	13	3,20	3,76	1,70	0,31	0,27	0,59
Sum				30	56	86	1,55	0,88	0,53	0,64	1,14	1,90

Location 2												
Strike W	Strike Fr.	Angle A-B	Length W	N 1'st	N 2'nd	N tot	Sp. N 1'st	Sp. N 2'nd	Sp. N tot	Fr. int.1	Fr. Int.2	Fr. Int tot
165	5	20	30	0	2	2	0,00	6,84	6,84	0,00	0,15	0,15
165	15	30	30	1	0	1	20,00	0,00	20,00	0,05	0,00	0,05
165	25	40	30	0	2	2	0,00	12,86	12,86	0,00	0,08	0,08
165	35	50	30	0	6	6	0,00	3,94	3,94	0,00	0,25	0,25
165	45	60	30	2	2	4	17,32	17,32	6,93	0,06	0,06	0,14
165	55	70	30	2	1	3	18,79	37,59	10,57	0,05	0,03	0,09
165	65	80	30	3	1	4	11,08	39,39	7,88	0,09	0,03	0,13
165	75	90	30	1	2	3	40,00	20,00	11,25	0,03	0,05	0,09
165	85	80	30	4	0	4	7,88	0,00	7,88	0,13	0,00	0,13
165	95	70	30	4	2	6	7,52	18,79	4,83	0,13	0,05	0,21
165	105	60	30	2	0	2	17,32	0,00	17,32	0,06	0,00	0,06
165	115	50	30	0	0	0	0,00	0,00	0,00	0,00	0,00	0,00
165	125	40	30	0	2	2	0,00	12,86	12,86	0,00	0,08	0,08
165	135	30	30	3	3	6	5,63	5,63	2,57	0,18	0,18	0,39
165	145	20	30	1	6	7	13,68	1,76	1,50	0,07	0,57	0,67
165	155	10	30	0	0	0	0,00	0,00	0,00	0,00	0,00	0,00
165	165	0	30	0	0	0	0,00	0,00	0,00	0,00	0,00	0,00
165	175	10	30	0	0	0	0,00	0,00	0,00	0,00	0,00	0,00
Sum				23	29	52	1,18	0,66	0,40	0,84	1,51	2,51

Location 3												
Strike W	Strike Fr.	Angle A-B	Length W	N 1'st	N 2'nd	N tot	Sp. N 1'st	Sp. N 2'nd	Sp. N tot	Fr. int.1	Fr. Int.2	Fr. Int tot
33	5	28	30	1	1	2	18,78	18,78	9,39	0,05	0,05	0,11
33	15	18	30	6	4	10	1,59	2,47	0,94	0,63	0,40	1,07
33	25	8	30	0	0	0	0,00	0,00	0,00	0,00	0,00	0,00
33	35	2	30	0	0	0	0,00	0,00	0,00	0,00	0,00	0,00
33	45	12	30	0	2	2	0,00	4,16	8,32	0,00	0,24	0,12
33	55	22	30	1	0	1	14,98	0,00	14,98	0,07	0,00	0,07
33	65	32	30	1	1	2	21,20	21,20	10,60	0,05	0,05	0,09
33	75	42	30	1	0	1	26,77	0,00	26,77	0,04	0,00	0,04
33	85	52	30	3	3	6	8,87	8,87	4,05	0,11	0,11	0,25
33	95	62	30	2	0	2	17,66	35,32	17,66	0,06	0,03	0,06
33	105	72	30	3	1	4	38,04	38,04	7,61	0,03	0,03	0,13
33	115	82	30	2	2	4	19,81	19,81	7,92	0,05	0,05	0,13
33	125	88	30	2	1	3	19,99	39,98	11,24	0,05	0,03	0,09
33	135	78	30	1	1	2	39,13	39,13	19,56	0,03	0,03	0,05
33	145	68	30	1	0	1	37,09	0,00	37,09	0,03	0,00	0,03
33	155	58	30	1	1	2	33,92	33,92	16,96	0,03	0,03	0,06
33	165	48	30	2	1	3	14,86	29,73	8,36	0,07	0,03	0,12
33	175	38	30	0	1	1	0,00	24,63	24,63	0,00	0,04	0,04
Sum				27	19	46	0,78	0,89	0,41	1,28	1,12	2,44

Location 4												
Strike W	Strike Fr.	Angle A-B	Length W	N 1'st	N 2'nd	N tot	Sp. N 1'st	Sp. N 2'nd	Sp. N tot	Fr. int.1	Fr. Int.2	Fr. Int tot
148	5	37	36	3	0	3	8,12	0,00	8,12	0,12	0,00	0,12
148	15	47	36	4	1	5	7,02	35,10	5,49	0,14	0,03	0,18
148	25	57	36	1	2	3	40,26	20,13	11,32	0,02	0,05	0,09
148	35	67	36	0	1	1	0,00	44,18	44,18	0,00	0,02	0,02
148	45	77	36	0	0	0	0,00	0,00	0,00	0,00	0,00	0,00
148	55	87	36	0	3	3	0,00	13,48	13,48	0,00	0,07	0,07
148	65	83	36	0	0	0	0,00	0,00	0,00	0,00	0,00	0,00
148	75	73	36	0	1	1	0,00	45,90	45,90	0,00	0,02	0,02
148	85	63	36	0	3	3	0,00	12,03	12,03	0,00	0,08	0,08
148	95	53	36	0	4	4	0,00	7,67	7,67	0,00	0,13	0,13
148	105	43	36	2	5	7	16,37	5,11	3,58	0,06	0,20	0,28
148	115	33	36	0	1	1	0,00	26,14	26,14	0,00	0,04	0,04
148	125	23	36	0	5	5	0,00	2,93	2,93	0,00	0,34	0,34
148	135	13	36	3	4	7	3,04	2,16	1,18	0,33	0,46	0,85
148	145	3	36	0	0	0	0,00	0,00	0,00	0,00	0,00	0,00
148	155	7	36	0	0	0	0,00	0,00	0,00	0,00	0,00	0,00
148	165	17	36	0	5	5	0,00	2,19	2,19	0,00	0,46	0,46
148	175	27	36	2	2	4	10,90	10,90	4,36	0,09	0,09	0,23
Sum				15,00	37,00	52,00	1,29	0,50	0,34	0,77	2,00	2,92

Location 6												
Strike W	Strike Fr.	Angle A-B	Length W	N 1'st	N 2'nd	N tot	Sp. N 1'st	Sp. N 2'nd	Sp. N tot	Fr. int.1	Fr. Int.2	Fr. Int tot
100	5	85	60	2	0	2	39,85	0,00	39,85	0,03	0,00	0,03
100	15	85	60	4	3	7	15,94	22,41	8,72	0,06	0,04	0,11
100	25	75	60	1	2	3	77,27	38,64	21,73	0,01	0,03	0,05
100	35	65	60	2	0	2	36,25	0,00	36,25	0,03	0,00	0,03
100	45	55	60	0	1	1	0,00	65,53	65,53	0,00	0,02	0,02
100	55	45	60	0	0	0	0,00	0,00	0,00	0,00	0,00	0,00
100	65	35	60	10	0	10	3,48	0,00	3,48	0,29	0,00	0,29
100	75	25	60	5	0	5	5,28	0,00	5,28	0,19	0,00	0,19
100	85	15	60	7	4	11	2,26	4,14	1,42	0,44	0,24	0,70
100	95	5	60	0	0	0	0,00	0,00	0,00	0,00	0,00	0,00
100	105	5	60	0	0	0	0,00	0,00	0,00	0,00	0,00	0,00
100	115	15	60	5	4	9	3,24	4,14	1,75	0,31	0,24	0,57
100	125	25	60	0	0	0	0,00	0,00	0,00	0,00	0,00	0,00
100	135	35	60	0	2	2	0,00	22,94	22,94	0,00	0,04	0,04
100	145	45	60	0	2	2	0,00	28,28	28,28	0,00	0,04	0,04
100	155	55	60	0	1	1	0,00	65,53	65,53	0,00	0,02	0,02
100	165	65	60	0	3	3	0,00	20,39	20,39	0,00	0,05	0,05
100	175	75	60	2	0	2	38,64	0,00	38,64	0,03	0,00	0,03
Sum				38	22	60	0,72	1,40	0,47	1,38	0,71	2,15

Location 7												
Strike W	Strike Fr.	Angle A-B	Length W	N 1'st	N 2'nd	N tot	Sp. N 1'st	Sp. N 2'nd	Sp. N tot	Fr. int.1	Fr. Int.2	Fr. Int tot
30	5	25	50	0	0	0	0,00	0,00	0,00	0,00	0,00	0,00
30	15	15	50	0	1	1	0,00	17,25	17,25	0,00	0,06	0,06
30	25	5	50	0	0	0	0,00	0,00	0,00	0,00	0,00	0,00
30	35	5	50	0	0	0	0,00	0,00	0,00	0,00	0,00	0,00
30	45	15	50	0	0	0	0,00	0,00	0,00	0,00	0,00	0,00
30	55	25	50	1	0	1	28,17	0,00	28,17	0,04	0,00	0,04
30	65	35	50	2	0	2	19,12	0,00	19,12	0,05	0,00	0,05
30	75	45	50	6	0	6	6,06	0,00	6,06	0,16	0,00	0,16
30	85	55	50	3	1	4	15,36	54,61	10,92	0,07	0,02	0,09
30	95	65	50	11	2	13	4,15	30,21	3,51	0,24	0,03	0,29
30	105	75	50	6	5	11	8,28	10,06	4,43	0,12	0,10	0,23
30	115	85	50	1	4	5	66,41	13,28	10,38	0,02	0,08	0,10
30	125	85	50	7	6	13	7,26	8,54	3,85	0,14	0,12	0,26
30	135	75	50	4	1	5	12,88	64,40	10,06	0,08	0,02	0,10
30	145	65	50	2	1	3	30,21	60,42	16,99	0,03	0,02	0,06
30	155	55	50	1	1	2	54,61	54,61	54,61	0,02	0,02	0,02
30	165	45	50	0	0	0	0,00	0,00	0,00	0,00	0,00	0,00
30	175	35	50	0	0	0	0,00	0,00	0,00	0,00	0,00	0,00
Sum				44	22	66	1,04	2,21	0,69	0,96	0,45	1,45

Location 8												
Strike W	Strike Fr.	Angle A-B	Length W	N 1'st	N 2'nd	N tot	Sp. N 1'st	Sp. N 2'nd	Sp. N tot	Fr. int.1	Fr. Int.2	Fr. Int tot
35	5	30	60	1	1	2	40,00	40,00	20,00	0,03	0,03	0,05
35	15	20	60	0	1	1	0,00	27,36	27,36	0,00	0,04	0,04
35	25	10	60	4	5	9	2,78	2,17	1,17	0,36	0,46	0,85
35	35	0	60	0	0	0	0,00	0,00	0,00	0,00	0,00	0,00
35	45	10	60	4	0	4	2,78	0,00	2,78	0,36	0,00	0,36
35	55	20	60	4	2	6	5,47	13,68	3,52	0,18	0,07	0,28
35	65	30	60	0	2	2	0,00	20,00	20,00	0,00	0,05	0,05
35	75	40	60	0	1	1	0,00	51,42	51,42	0,00	0,02	0,02
35	85	50	60	2	2	4	30,64	30,64	12,26	0,03	0,03	0,08
35	95	60	60	3	6	9	19,49	8,91	5,85	0,05	0,11	0,17
35	105	70	60	7	5	12	8,22	11,75	4,73	0,12	0,09	0,21
35	115	80	60	5	3	8	12,31	22,16	7,50	0,08	0,05	0,13
35	125	90	60	7	5	12	8,75	12,50	5,03	0,11	0,08	0,20
35	135	80	60	2	3	5	39,39	22,16	12,31	0,03	0,05	0,08
35	145	70	60	3	5	8	21,14	11,75	7,16	0,05	0,09	0,14
35	155	60	60	1	8	9	69,28	6,60	5,85	0,01	0,15	0,17
35	165	50	60	2	2	4	30,64	30,64	12,26	0,03	0,03	0,08
35	175	40	60	0	1	1	0,00	51,42	51,42	0,00	0,02	0,02
Sum				45	52	97	0,69	0,74	0,34	1,45	1,35	2,94

Location 9												
Strike W	Strike Fr.	Angle A-B	Length W	N 1'st	N 2'nd	N tot	Sp. N 1'st	Sp. N 2'nd	Sp. N tot	Fr. int.1	Fr. Int.2	Fr. Int tot
103	5	78	30	1	1	2	39,13	39,13	19,56	0,03	0,03	0,05
103	15	88	30	0	0	0	0,00	0,00	0,00	0,00	0,00	0,00
103	25	82	30	0	0	0	0,00	0,00	0,00	0,00	0,00	0,00
103	35	72	30	0	0	0	0,00	0,00	0,00	0,00	0,00	0,00
103	45	62	30	0	1	1	0,00	35,32	35,32	0,00	0,03	0,03
103	55	52	30	2	0	2	15,76	0,00	15,76	0,06	0,00	0,06
103	65	42	30	8	2	10	2,55	13,38	2,03	0,39	0,07	0,49
103	75	32	30	12	1	13	1,33	21,20	1,23	0,75	0,05	0,81
103	85	22	30	12	2	14	0,94	7,49	0,81	1,06	0,13	1,24
103	95	12	30	3	6	9	2,34	1,07	0,70	0,43	0,94	1,43
103	105	2	30	0	0	0	0,00	0,00	0,00	0,00	0,00	0,00
103	115	8	30	0	0	0	0,00	0,00	0,00	0,00	0,00	0,00
103	125	18	30	2	0	2	6,18	0,00	6,18	0,16	0,00	0,16
103	135	28	30	1	2	3	18,78	9,39	5,28	0,05	0,11	0,19
103	145	38	30	1	5	6	24,63	3,85	3,17	0,04	0,26	0,32
103	155	48	30	1	1	2	29,73	29,73	14,86	0,03	0,03	0,07
103	165	58	30	0	0	0	0,00	0,00	0,00	0,00	0,00	0,00
103	175	68	30	0	0	0	0,00	0,00	0,00	0,00	0,00	0,00
Sum				43	21	64	0,33	0,61	0,21	3,01	1,64	4,85